Visible light-induced photoisomerization of indole-oxindole constructs: Molecular disassembly and ROS-mediated apoptosis

Kartikay Tyagi [a], Tejal Dixit[a], and V. Venkatesh*[a]

[a] Laboratory of Chemical Biology and Medicinal Chemistry, Department of Chemistry, Indian Institute of Technology Roorkee, Uttarakhand-247667, India, E-mail: venkatesh.v@cy.iitr.ac.in

Table of Contents **Page No.**

1.1 General Experimental Details: All solvents and reagents were used as received from the suppliers. TLC was performed on Merck Kiesel gel 60, F_{254} plates with a layer thickness of 0.25 mm. Column chromatography was performed on silica gel (100-200 mesh) using a gradient of ethyl acetate and hexane as mobile phase. ^{1}H NMR spectral data were collected at 500 MHz (JEOL), ^{13}C NMR was recorded at 126 MHz, and ^{31}P NMR was recorded at 202 MHz. ^{1}H NMR spectral data are given as chemical shifts in ppm followed by multiplicity (s- singlet; d- doublet; t- triplet; q- quartet; m- multiplet), number of protons, and coupling constants. ^{13}C NMR and ^{31}P NMR chemical shifts are expressed in ppm. UV−visible absorption data were collected on a Shimadzu UV-2600 UV/vis/NIR spectrophotometer. Fluorescence spectra were recorded using Horiba FluoroMax Plus spectrofluorometer. Results obtained from all the cellular assays were recorded by BioTek synergy H1 plate reader. Cellular imaging experiments were performed using an Olympus fluorescence-inverted microscope. All the flow cytometry experiments were conducted using the BD FACS instrument and analysed by BD FACSDiva 8.0.3 software. PLQY was determined with Horiba Scientific FluoroMax TCSPC Spectrofluorometer equipped with the integrating sphere.

Materials: All reactions were carried out under an inert atmosphere, in oven-dried glassware, unless otherwise stated. Dimethylformamide (DMF), and dimethyl sulphoxide (DMSO) were dried, degassed, and stored under an atmosphere of nitrogen before use. Ethanol was used as obtained from the supplier. Indole-3-carboxaldehyde and 2-oxindole were purchased from TCI. 1,2-dibromoethane, 4-bromo-N, N-dimethylaniline, and 4-nitrobenzene sulfonyl chloride were purchased from Alfa Aeser. Cu_2O and 5,5-dimethyl-1-pyrroline-N-oxide (DMPO) were bought from Sigma Aldrich, and potassium carbonate was purchased from SRL.

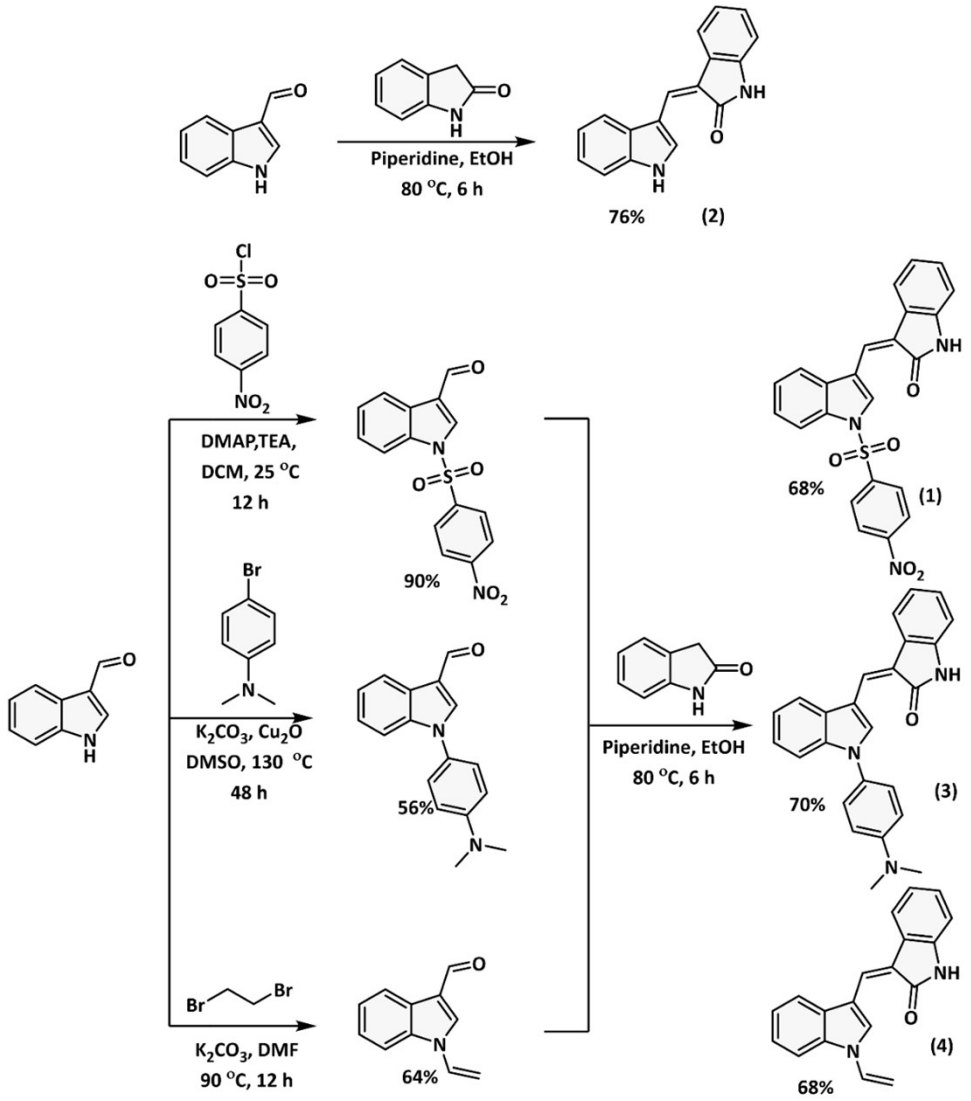

Fig. S1: Synthesized indole-oxindole hybrids accompanying different functionalities at indole nitrogen.

Synthesis of precursor aldehydes

Aldehyde 1

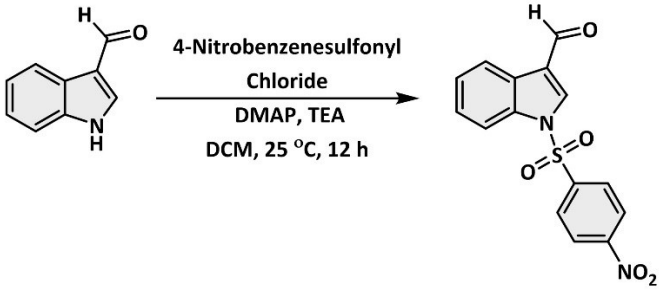

Synthesis of aldehyde 1: Synthesis of aldehyde 1 was achieved by following the reported literature protocol.[1] Indole-3-carboxaldehyde (200 mg, 1.37 mmol, 1 equiv.), 4-Dimethyaminopyridine (DMAP) (13. 4 mg, 0.110 mmol, 0.08 equiv.), and triethylamine (287 µL, 2.06 mmol, 1.5 equiv.) were dissolved in 5 mL DCM. Furthermore, 4-nitrobenzene sulfonyl chloride (366 mg, 1.65 mmol, 1.2 equiv.) was added in portions into the reaction mixture and was allowed to stir at 25 °C for 12 h. After completion of the reaction, the reaction mixture was diluted with 10 mL DCM and quenched with aq. HCl (15 mL, 5%). The organic layer was separated and dried over anhydrous sodium sulphate and evaporated. The crude product was redissolved in 10 mL DCM and passed through a short silica plug to obtain pure product as an off-white solid (Yield 90%). ^{1}H NMR (500 MHz, $CDCl_3$) δ 10.07 (d, J = 11.1 Hz, 1H), 8.30 (t, J = 9.2 Hz, 2H), 8.21 (s, 2H), 8.12 (t, J = 6.0 Hz, 2H), 7.90 (t, J = 10.9 Hz, 1H), 7.44 – 7.29 (m, 2H).^{13}C NMR (126 MHz, $CDCl_3$) δ 185.26 (s), 151.14 (s), 142.58 (s), 135.69 (s), 135.09 (s), 128.58 (s), 126.98 (s), 126.49 (s), 125.76 (s), 124.94 (s), 123.45 (s), 123.02 (s), 113.05 (s).

Aldehyde 2

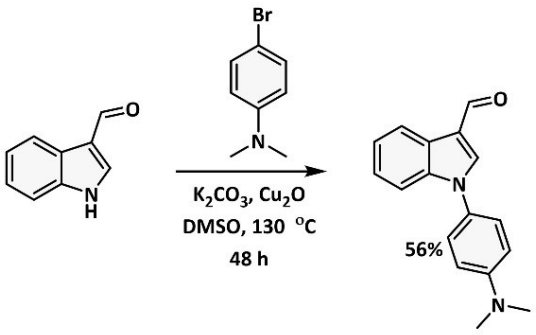

Synthesis of aldehyde 2 was performed by following the reported literature protocol with slight modifications.[2] In an oven-dried Schlenk tube, indole-3-carboxaldehyde (100 mg, 0.68 mmol, 1 equiv.), 4-bromo-N,N-dimethylaniline (303 mg, 1.51 mmol, 2.2 equiv.), and potassium carbonate (235 mg, 1.7 mmol, 2.5 equiv.) were dissolved in 10 mL DMSO. Cu_2O (20 mg, 0.136 mmol, 0.2 equiv.) was added subsequently, and the reaction mixture was allowed to stir at 130 °C for 48 h. After completion of the reaction, the reaction mixture was poured into cold water and extracted with ethyl acetate. The organic layer was dried under reduced pressure, and the pure product was collected by column chromatography (ethyl acetate/hexane 30:70) as a brown solid (Yield 58%). ^{1}H NMR (500 MHz, $CDCl_3$) δ 10.07 (s, 1H), 8.39 – 8.30 (m, 1H), 7.83 (s, 1H), 7.41 – 7.38 (m, 1H), 7.35 – 7.33 (m, 2H), 7.31 (dd, *J* = 4.0, 1.6 Hz, 2H), 6.84 – 6.78 (m, 2H), 3.04 (s, 6H). ^{13}C NMR (126 MHz, $CDCl_3$) δ 184.97 (s), 150.32 (s), 138.92 (s), 138.30 (s), 126.88 (s), 126.07 (s), 125.35 (s), 124.26 (s), 123.17 (s), 122.11 (s), 119.00 (s), 112.71 (s), 111.34 (s), 40.61 (s). HRMS (ESI): Calculated for $[M+H]^+$ m/z: 265.1335, Found: 265.1339.

Aldehyde 3

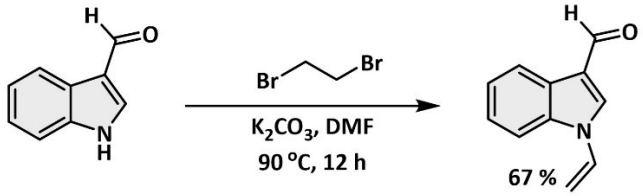

Precursor aldehyde 3 was prepared by following the reported literature.[3] Indole-3-carboxaldehyde (250 mg, 1.72 mmol, 1 equiv.), 1,2-dibromoethane (298 µL, 3.44 mmol, 2 equiv.) and potassium carbonate (522 mg, 3.78 mmol, 2.20 equiv.) in DMF (8 mL) were taken in a round bottom flask, and the reaction mixture was allowed to stir at 90 °C for 12 h. After completion of the reaction, the reaction mixture was poured into ice-cold water and extracted with ethyl acetate. The combined organic layer was evaporated under reduced pressure and further pure n-vinyl indole was isolated through column chromatography (ethyl acetate/hexane 10:90) as a pale-yellow oil (Yield 67%). ^{1}H NMR (500 MHz, $CDCl_3$) δ 10.08 (s, 1H), 8.39 – 8.20 (m, 1H), 8.00 (s, J = 20.4 Hz, 1H), 7.51 – 7.46 (m, 2H), 7.40 – 7.29 (m, 1H), 7.23 – 7.18 (m, 1H), 5.47 (dd, J = 15.7, 1.9 Hz, 1H), 5.08 (dd, J = 8.9, 1.9 Hz, 1H). ^{13}C NMR (126 MHz, $CDCl_3$) δ 185.15 (s), 136.68 (s), 133.66 (s), 129.23 (s), 125.53 (s), 124.91 (s), 123.77 (s), 122.39 (s), 120.17 (s), 110.07 (s), 102.27 (s).

General synthesis of indole-oxindole constructs (IOCs)

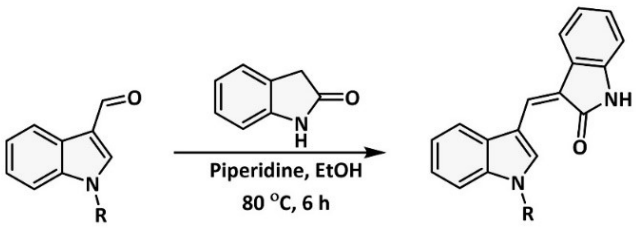

All the indole-oxindole constructs (IOCs) were prepared by a straightforward Knoevenagel condensation reaction. Corresponding aldehyde (1equiv.), 2-oxindole (1.1 equiv.) was dissolved in ethanol along with a catalytic amount of piperidine (0.1 equiv.), and reaction content was refluxed at 80 °C for 6 h. After that the reaction mass was allowed to get cool.

The obtained product as a yellow colour precipitate was collected from filtration, washed with ethanol, and dried in air.

IOC-1-Z: ^{1}H NMR (500 MHz, DMSO-d_6) δ 10.74 (s, 1H), 9.71 (s, 1H), 8.34 (d, J = 9.1 Hz, 2H), 8.28 – 8.22 (m, 3H), 7.98 (d, J = 10.5 Hz, 2H), 7.92 (d, J = 7.5 Hz, 1H), 7.43 (dt, J = 14.8, 7.2 Hz, 2H), 7.20 (t, J = 7.1 Hz, 1H), 6.98 (t, J = 7.5 Hz, 1H), 6.85 (d, J = 7.7 Hz, 1H).^{13}C NMR (126 MHz, DMSO-d_6) δ 168.14 (s), 151.41 (s), 141.76 (s), 140.94 (s), 133.99 (s), 131.11 (s), 130.95 (s), 129.62 (s), 129.02 (s), 127.32 (s), 126.45 (s), 125.91 (s), 124.98 (s), 124.83 (s), 123.46 (s), 121.60 (s), 120.93 (s), 120.75 (s), 117.24 (s), 113.66 (s), 110.07 (s). HRMS Calculated for $[M+H]^+$ m/z: 446.0805, Found: 446.0809.

IOC-2-Z: ^{1}H NMR (500 MHz, DMSO-d_6) δ 11.97 (s, 1H), 10.48 (s, 1H), 9.42 (d, J = 2.8 Hz, 1H), 8.13 (dd, J = 5.1, 2.7 Hz, 1H), 8.11 (s, 1H), 7.84 (d, J = 7.2 Hz, 1H), 7.51 – 7.46 (m, 1H), 7.22 – 7.18 (m, 2H), 7.10 (td, J = 7.6, 1.1 Hz, 1H), 6.98 – 6.91 (m, 1H), 6.81 (d, J = 7.6 Hz, 1H). ^{13}C NMR (126 MHz, DMSO-d_6) δ 168.62 (s), 139.67 (s), 136.39 (s), 134.04 (s), 128.73 (s), 127.69 (s), 127.28 (s), 126.20 (s), 123.03 (s), 121.28 (s), 121.05 (s), 119.62 (s), 119.23 (s), 118.95 (s), 112.79 (s), 111.78 (s), 109.48 (s), 109.48 (s). HRMS Calculated for $[M+H]^+$ m/z: 261.1022, Found: 261.1026.

IOC-3-Z: ^{1}H NMR (500 MHz, $CDCl_3$) δ 9.55 (s, 1H), 8.74 (s, 1H), 7.96 (s, 1H), 7.92 (d, *J* = 8.1 Hz, 1H), 7.58 (d, *J* = 7.6 Hz, 1H), 7.45 (d, *J* = 5.4 Hz, 1H), 7.38 (d, *J* = 10.5 Hz, 2H), 7.28 (t, *J* = 8.7 Hz, 1H), 7.23 (d, *J* = 5.8 Hz, 1H), 7.11 (t, *J* = 7.6 Hz, 1H), 7.00 (t, *J* = 6.8 Hz, 1H), 6.84 (d, *J* = 7.1 Hz, 1H), 6.78 (d, *J* = 10.2 Hz, 2H), 2.99 (s, 6H). ^{13}C NMR (126 MHz, $CDCl_3$) δ 168.91 (s), 150.00 (s), 138.74 (s), 136.95 (s), 136.67 (s), 129.42 (s), 127.83 (s), 126.93 (s), 126.67 (s), 126.16 (s), 125.88 (s), 123.08 (s), 121.69 (s), 121.20 (s), 119.61 (s), 118.12 (s, J = 8.2 Hz), 118.05 (s), 112.75 (s), 112.00 (s), 111.55 (s), 109.38 (s), 40.67 (s). HRMS Calculated for $[M+H]^+$ m/z: 380.1757, Found: 380.1757.

IOC-4-Z ^{1}H NMR (500 MHz, DMSO-d_6) δ 10.60 (s, 1H), 9.69 (s, 1H), 8.20 (d, , *J* = 7.3 Hz, 1H), 8.08 (s, 1H), 7.89 (d, *J* = 7.5 Hz, 1H), 7.78 (d, *J* = 7.6 Hz, 1H), 7.60 (dd, *J* = 15.6, 8.9 Hz, 1H), 7.40 – 7.24 (m, 2H), 7.15 (t, *J* = 8.1 Hz, 1H), 6.97 (t, *J* = 7.6 Hz, 1H), 6.84 (d, *J* = 7.7 Hz, 1H), 5.44 (dd, *J* = 15.5, 1.3 Hz, 1H), 5.02 (dd, *J* = 8.8, 1.4 Hz, 1H). ^{13}C NMR (126 MHz, DMSO-d_6) δ 168.46 (s), 140.17 (s), 135.65 (s), 130.31 (s), 130.07 (s), 129.47 (s), 128.23 (s), 125.87 (s), 125.65 (s), 124.32 (s), 122.68 (s), 122.58 (s), 121.36 (s), 119.91 (s), 119.59 (s), 113.67 (s), 111.30 (s), 109.78 (s), 100.71 (s). HRMS Calculated for $[M+H]^+$ m/z: 287.1179, Found: 287.1184.

IOC-4-E: ^{1}H NMR (500 MHz, DMSO-d_6) δ 10.54 (s, 1H), 8.49 (s, 1H), 7.82 (d, J = 8.3 Hz, 1H), 7.77 (s, 1H), 7.59 (dd, J = 15.7, 11.3 Hz, 3H), 7.33 (t, J = 8.0 Hz, 1H), 7.23 (t, J = 7.5 Hz, 1H), 7.17 (t, J = 7.6 Hz, 1H), 6.87 (dd, J = 12.5, 7.7 Hz, 2H), 5.64 (dd, J = 15.6, 1.3 Hz, 1H), 4.96 (dd, J = 8.9, 1.3 Hz, 1H). ^{13}C NMR (126 MHz, DMSO-d_6) δ 169.71 (s), 142.71 (s), 135.98 (s), 130.12 (s), 129.62 (s), 128.14 (s), 127.26 (s), 126.66 (s), 125.11 (s), 124.42 (s), 123.24 (s), 122.54 (s), 122.27 (s), 121.63 (s), 120.28 (s), 113.44 (s), 111.60 (s), 110.23 (s), 100.63 (s). HRMS Calculated for $[M+H]^+$ m/z: 287.1179, Found: 287.1178.

Cell lines and culture maintenance

Human cervical cancer cells (HeLa), human prostate cancer cells (PC3), human colorectal cancer cells (HCT-116), human melanoma cells (A-375), and Human Embryonic Kidney cells (HEK-293) were bought from NCCS (National Centre for Cell Science), Pune, Maharashtra, India. Human lung cancer cells (A549) were purchased from ATCC (American Type Culture Collection) Washington, DC, USA. All the cells were grown in Dulbecco's Modified Eagle Medium (DMEM) along with 2.2 g/L sodium bicarbonate, 10% Fetal bovine serum (FBS), penicillin G (100 units/mL), and streptomycin (100 mg/mL). All the cells were cultured at approx. 80-90% confluence and further sub-cultured as an adherent monolayer in a humidified incubator at 37 ˚C with 5% CO_2 in different-sized cell culture dishes/ plates, depending on the type of experiment.

XRD analysis of synthesized IOCs

Bright, yellow-coloured fluorescent crystals of all the IOCs were obtained by slow evaporation technique from the mixture of toluene and DCM (98:2, v/v). The X-ray data collection and processing were performed on a Bruker Kappa Apex-II CCD diffractometer (Mo Kα λ = 0.71073). The crystal data for IOC-1-Z and IOC-2-Z was collected at 300 K. However, the crystal data for IOC-3-Z, IOC-4-Z, and IOC-4-E was collected at 100K. The structure was solved by using the direct method with the help of olex2. Final images were created using the Diamond program. The H atoms were placed in ideal calculated positions and refined as riding atoms with relative isotropic displacement parameters. Crystal data, data collection parameters, and structure refinement details are given in Table S1-S5.

XRD analysis of IOC-1-Z

Table S1

Crystal data and structure refinement forVV_KT_788_1289_0m. Identification code	VV_KT_788_1289_0m
CCDC No.	2388040
Empirical formula	$C_{92}H_{60}N_{12}O_{20}S_4$
Formula weight	1781.76
Temperature/K	300.0
Crystal system	monoclinic
Space group	$P2_1/c$
a/Å	38.655(9)
b/Å	9.417(2)
c/Å	22.232(5)
α/°	90
β/°	93.433(6)
γ/°	90
Volume/Å3	8078(3)
Z	4
ρ_{calc}g/cm3	1.465
μ/mm-1	0.203
F(000)	3680.0
Crystal size/mm3	0.152 × 0.116 × 0.076
Radiation	MoKα (λ = 0.71073)
2Θ range for data collection/°	3.166 to 50.822
Index ranges	-46 ≤ h ≤ 46, -11 ≤ k ≤ 11, -26 ≤ l ≤ 26
Reflections collected	180302

Independent reflections	14602 [Rint = 0.1071, Rsigma = 0.0636]
Data/restraints/parameters	14602/0/1153
Goodness-of-fit on F2	1.024
Final R indexes [I>=2σ (I)]	R1 = 0.0650, wR2 = 0.1790
Final R indexes [all data]	R1 = 0.1145, wR2 = 0.2203
Largest diff. peak/hole / e Å-3	0.47/-0.38

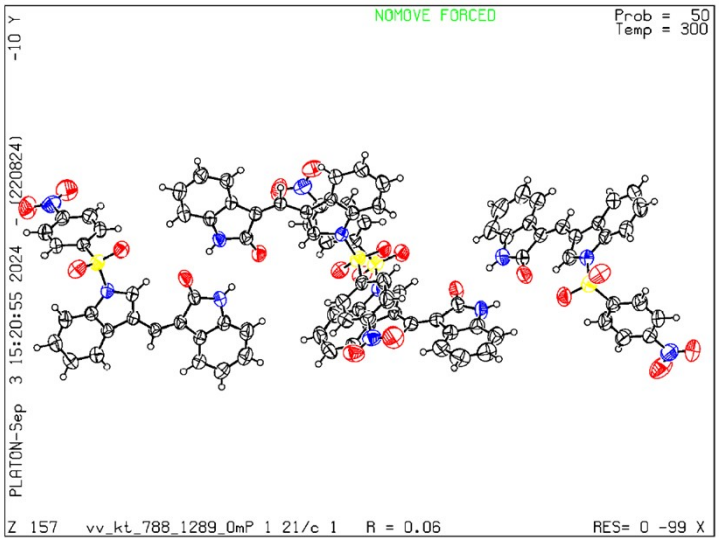

XRD analysis of IOC-2-Z

Table S2

vv_kt_769_1288_0m Table 2 Crystal data and structure refinement forvv_kt_769_1288_0m. Identification code	vv_kt_769_1288_0m
CCDC No.	2388038
Empirical formula	C17H14N2O2
Formula weight	278.30
Temperature/K	300.00
Crystal system	monoclinic
Space group	C2/c
a/Å	29.648(7)
b/Å	6.1467(14)
c/Å	15.396(4)
α/°	90
β/°	101.548(7)
γ/°	90
Volume/Å3	2748.9(11)
Z	8
ρcalcg/cm3	1.345
μ/mm-1	0.090

F(000)	1168.0
Crystal size/mm3	0.588 × 0.204 × 0.066
Radiation	MoKα (λ = 0.71073)
2Θ range for data collection/°	5.402 to 50.112
Index ranges	-34 ≤ h ≤ 34, -7 ≤ k ≤ 7, -18 ≤ l ≤ 18
Reflections collected	34672
Independent reflections	2436 [Rint = 0.0389, Rsigma = 0.0205]
Data/restraints/parameters	2436/0/193
Goodness-of-fit on F2	1.066
Final R indexes [I>=2σ (I)]	R1 = 0.0372, wR2 = 0.0973
Final R indexes [all data]	R1 = 0.0401, wR2 = 0.1000
Largest diff. peak/hole / e Å-3	0.15/-0.16

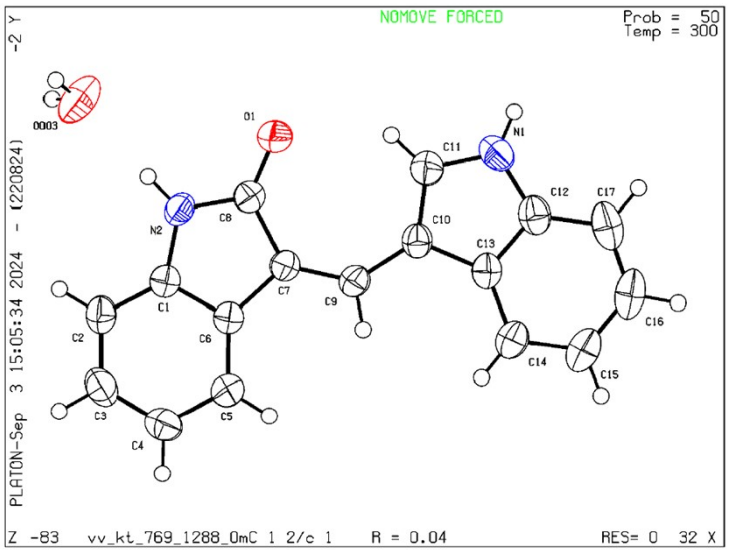

XRD analysis of IOC-3-Z

Table S3

forVV_KT_777_1255_0m. Identification code	VV_KT_777_1255_0m
CCDC No.	2388192
Empirical formula	C51H43Cl3N6O2
Formula weight	878.26
Temperature/K	100.00
Crystal system	monoclinic
Space group	P21/n
a/Å	19.8975(9)
b/Å	7.5952(3)
c/Å	28.4543(12)
α/°	90

β/°	95.4050(10)
γ/°	90
Volume/Å3	4281.0(3)
Z	4
ρcalcg/cm3	1.363
μ/mm-1	0.264
F(000)	1832.0
Crystal size/mm3	0.147 × 0.094 × 0.032
Radiation	MoKα (λ = 0.71073)
2Θ range for data collection/°	4.112 to 53.508
Index ranges	-25 ≤ h ≤ 24, -9 ≤ k ≤ 9, -35 ≤ l ≤ 36
Reflections collected	112728
Independent reflections	9074 [Rint = 0.0932, Rsigma = 0.0582]
Data/restraints/parameters	9074/0/563
Goodness-of-fit on F2	1.015
Final R indexes [I>=2σ (I)]	R1 = 0.0542, wR2 = 0.1370
Final R indexes [all data]	R1 = 0.0969, wR2 = 0.1638
Largest diff. peak/hole / e Å-3	0.52/-0.45

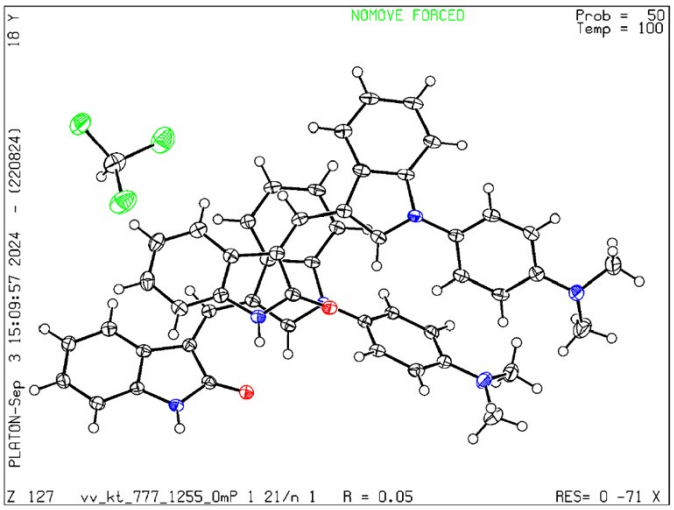

XRD analysis of IOC-4-Z

Table S4

VV_KT_784_1026_0m Table 1 Crystal data and structure refinement forVV_KT_784_1026_0m. Identification code	VV_KT_784_1026_0m
CCDC No.	2388193
Empirical formula	C9.5H7NO0.5
Formula weight	143.16
Temperature/K	100.0
Crystal system	monoclinic
Space group	P21

a/Å	10.576(4)
b/Å	4.7113(16)
c/Å	14.303(5)
α/°	90
β/°	102.737(13)
γ/°	90
Volume/Å3	695.1(4)
Z	4
ρcalcg/cm3	1.368
μ/mm-1	0.086
F(000)	300.0
Crystal size/mm3	0.385 × 0.019 × 0.014
Radiation	MoKα (λ = 0.71073)
2Θ range for data collection/°	3.948 to 49.088
Index ranges	-12 ≤ h ≤ 12, -5 ≤ k ≤ 5, -16 ≤ l ≤ 16
Reflections collected	7573
Independent reflections	2326 [Rint = 0.1125, Rsigma = 0.1515]
Data/restraints/parameters	2326/1/207
Goodness-of-fit on F2	1.002
Final R indexes [I>=2σ (I)]	R1 = 0.0792, wR2 = 0.1495
Final R indexes [all data]	R1 = 0.1436, wR2 = 0.1728
Largest diff. peak/hole / e Å-3	0.28/-0.29
Flack parameter	-0.7(10)

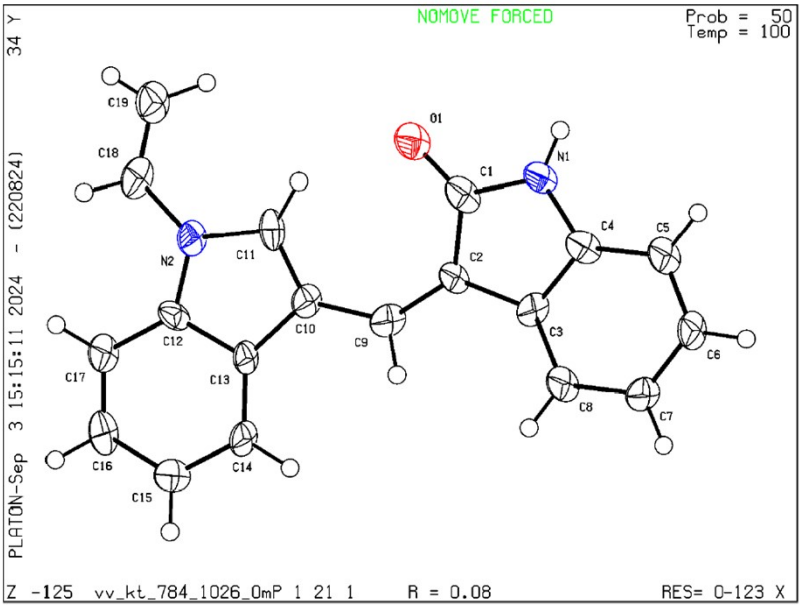

XRD analysis of IOC-4-E

Table S5

VV_KT_784E_1303_0m Table 1 Crystal data and structure refinement forVV_KT_784E_1303_0m. Identification code	VV_KT_784E_1303_0m
CCDC No.	2388039
Empirical formula	$C_{19}H_{14}N_2O$
Formula weight	286.32
Temperature/K	100.0
Crystal system	monoclinic
Space group	$P2_1/n$
a/Å	17.846(3)
b/Å	3.9434(7)
c/Å	19.519(3)
α/°	90
β/°	97.487(6)
γ/°	90
Volume/Å^3	1361.9(4)
Z	4
ρ_{calc}g/cm^3	1.396
μ/mm^{-1}	0.088
F(000)	600.0
Crystal size/mm^3	0.307 × 0.093 × 0.031
Radiation	MoKα (λ = 0.71073)
2Θ range for data collection/°	4.21 to 50.2
Index ranges	-21 ≤ h ≤ 20, -4 ≤ k ≤ 4, -23 ≤ l ≤ 23
Reflections collected	26009
Independent reflections	2430 [R_{int} = 0.0748, R_{sigma} = 0.0519]
Data/restraints/parameters	2430/0/207
Goodness-of-fit on F^2	1.027
Final R indexes [I>=2σ (I)]	R_1 = 0.0447, wR_2 = 0.1048
Final R indexes [all data]	R_1 = 0.0644, wR_2 = 0.1161
Largest diff. peak/hole / e Å^{-3}	0.22/-0.20

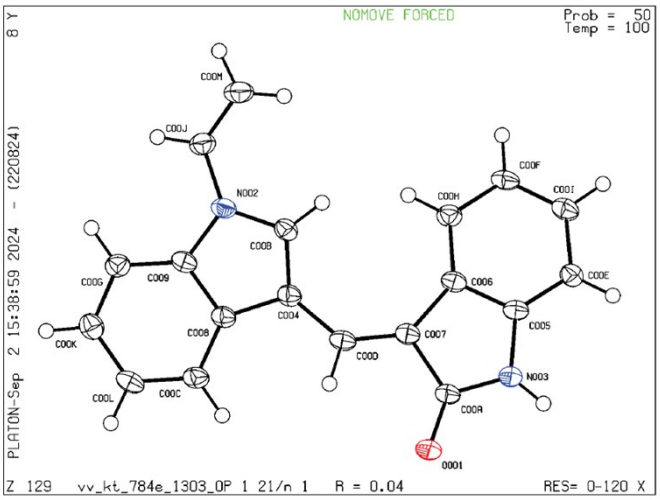

EPR Analysis

The EPR experiment was performed at room temperature (298 K) on a Bruker Biospin EMX micro A200 spectrometer. Field modulation was given at 100 kHz and 0.05 mT, and the microwave attenuation was 0.657 mW with a microwave frequency of 9.390 GHz. The IOC-4-Z (200 µm) in acetonitrile was placed in a capillary positioned in a cavity. Irradiation was executed with a 450 nm LED source. The following EPR parameters were used to acquire the spectra: sweep width of 5 mT, 1024 points, time constant of 163.84 ms, and conversion time of 75 ms, providing a sweep time of ∼76 s. The spin trap DMPO (30 mM) was used to capture and identify the formation of different ROS produced by IOC-4-Z after irradiation with 450 nm LED for 20 min.

Determination of PLQY

The PLYQ of the samples was performed using a Horiba Scientific FluoroMax TCSPC Spectrofluorometer equipped with the integrating sphere. An intensity-modulated 300 W Xe-lamp light source was used for excitation. For the measurements, the samples were fabricated as a thin film and were dispersed in ethanol and then deposited on a quartz substrate. All the films were dried and used further for the measurements (λ_{ex} = 470 nm) with their respective emission wavelengths. All the PLQY measurements were carried out in the air at room temperature. The measurements were recorded with respect to the blank substrate so that we get the PLQY values for samples only.

Cell viability assay

The cell viability was determined using a 3-(4,5-dimethylthiazolyl-2)-2,5-diphenyltetrazolium bromide (MTT) assay. Briefly, 10,000 cells per well were seeded in 96 well culture plates and grown for 24 h. The stock solution (10 mM) of synthesized molecules was prepared in DMSO and further diluted with media (with FBS) so that the final concentration of DMSO in all the wells was lower than 0.4%. All the prepared solutions were added to the cells and kept for 24 h incubation. After 24 h of incubation, phosphate-buffered saline (PBS) was added to both plates after the previous media had been removed. The light plate was then irradiated with an LED source (456 nm, 30 mW/cm^2) for 45 min. Simultaneously, the dark plate was kept in the dark with PBS for 45 min (without irradiation). After removing PBS, media (with FBS, 200 µL/well) is added in all wells and incubated for another 24 h. The cells were then washed further with PBS and incubated with a freshly prepared 10 µL (5 mg/mL) MTT in 100 µL media (without FBS) for 4 h at 37 °C. After 4 h, 50 µL of media is removed carefully without disturbing the formazan crystal, and 150 µL of DMSO is added to each well. Using a microplate reader, the absorbance was measured at 570 nm, and cell viability was calculated by comparing the absorbance of IOCs treated cells with the untreated cells (cells alone).

Detection and quantification of intracellular ROS

Intracellular ROS levels were detected and measured by the fluorescent probe DCFH-DA using the slight modification reported in the literature.[3] Cells were treated with IOC-4-Z and IOC-4-E (25 µM) for 4 h; after that, the culture medium was removed, and IOC-4-Z treated cells were subjected to an LED light source (456 nm, 30 mW/cm2) for 30 min. Furthermore, cells were washed with 1X PBS and then incubated with DCFH-DA (20 µM) at 37 °C for 20 min under dark conditions. Hydrogen peroxide (working conc. 25 µM) was considered as a positive control. Cells were then washed with 1X PBS (1 mL) twice, and then images were captured in green channels and bright fields with the help of an Olympus fluorescence inverted microscope. All the images were taken at the same exposure time. After imaging, cells were trypsinised, collected, and centrifuged to make pellets that were further suspended in PBS. The fluorescence intensities were quantified by using a microplate reader with excitation (485 nm) and emission (535 nm), respectively. The obtained results were plotted as a mean DCF fluorescence intensity corresponding to the ROS generation.

DAPI Staining for nuclear stress analysis

5×10^4 HCT 116 cells were seeded on Poly-D-lysine-coated coverslips and allowed to grow for 24 h under a humidified atmosphere with 5% CO_2. Furthermore, cells were incubated with IOC-4-Z and IOC-4-E (25 µM) for 4h. After that, the culture medium was taken out, and PBS was added to the cells, which were further irradiated for 30 minutes. Furthermore, PBS was removed, and a media containing FBS was added to the cells, which were again incubated for 4 h. Furthermore, media was removed from the cells, and then the cells were fixed with 4% paraformaldehyde for 10 minutes. Cells were carefully washed again with PBS and permeabilized by 0.1% Triton X-100 for 10 min. Furthermore, cells were washed again with PBS and incubated with DAPI (1µg/mL in PBS) for 30 min under dark conditions. After 30 min, cells were washed twice with PBS, and images were captured with the help of a fluorescence microscope under a blue channel.

JC-1 staining for the detection of Mitochondrial Membrane Potential (MMP)

Mitochondrial membrane potential (MMP, ΔΨm) was analysed by using HCT 116 cells. Typically, 5×10^4 cells were seeded on Poly-D-lysine-coated coverslips and allowed to grow for 24 h under humidified conditions at 37 °C with 5% CO_2. Cells were then incubated with IOC-4-Z and IOC-4-E for 4 h. After 4 h, media containing IOCs was removed, and PBS was added to the cells and further subjected to light irradiation for 30 min. The cells were washed with PBS and incubated with JC-1 (5µg/mL) for 30 min in the dark. Furthermore, the dye was removed, cells were washed with PBS, and images were captured with the help of an Olympus fluorescence microscope under bright field, green, and red channels with constant exposure time and fluorescence intensity.

Cell Apoptosis Assay

Cell apoptosis assay using Annex V FITC/PI was performed following the reported literature with slight modification.[5] Typically, 1×10^5 HCT 116 cells/well were seeded into 6-well plates and allowed to grow for 24 h under humidified conditions at 37 °C with 5% CO_2. After that, Cells were treated with IOC-4-Z and IOC-4-E (5 μM) for 5 h. Subsequently, cells were subjected to irradiation, and then cells were harvested and washed twice with ice-cold PBS, followed by annexin-V FITC/PI staining in annexin-V binding buffer for 15 min in the dark at room temperature, and analysed by using a flow cytometer.

FDA/PI Co-staining

5×10^4 cells were grown over poly-D lysine-coated coverslips for 24 h under a humidified atmosphere at 37 °C with 5% CO_2. After that, cells were treated with IOC-4-Z and IOC-4-E (25 μM) for 12 h. After completion of 12 h, the light group was subjected to irradiation for 30 min. and further kept for recovery for another 12 h. After that, the medium was removed, cells were gently washed with PBS, and cells were incubated in the dark with FDA (8 μg/mL) and PI (2 μg/mL) for 15 min. Then, cells were washed with 1X PBS twice, and then coverslips were mounted over the glass slides to capture the images using an Olympus fluorescence microscope.

DFT Analysis

Density functional theory was performed using Gaussian 16W software to calculate the energy of the highest occupied molecular orbital (HOMO) and lowest unoccupied molecular orbital (LUMO). The geometries of IOC-4-Z and IOC-4-E were optimized using the MP2 method with basis set 6-311++G(D, P).

Statistical analysis

Data are represented as mean ± SEM and statistical significance was evaluated by one-way and two-way analysis of variance (ANOVA) using Graph Pad Prism 5.0. Tukey's multiple comparison test to compare the means. Also, a p-value of less than 0.05 was considered significant.

3D Spheroid formation and imaging

3D Spheroids were formed using Corning ultra-low attachment 96 well plates. Typically, 2×10^4 cells were seeded per well, and spheroids were allowed to form for 72 h. After that, spheroids were treated with IOC-4-Z and IOC-4-E (25 µM) for 24 h, and then the culture medium was removed, and PBS was added for the subsequent irradiation for 30 min. After irradiation, spheroids were kept for 24 h recovery time in a cell culture medium. Furthermore, images were captured for 5 days.

Similarly, after 24 h recovery time, spheroids were incubated with FDA and PI for 10 minutes, washed carefully with PBS, and subjected to fluorescence microscopic analysis using an Olympus Fluorescence microscope.

Cellular Imaging by IOC-4-Z

5×10^4 cells were allowed to grow over lysine-coated coverslips for 24 h. After that, cells were incubated with IOC-4-Z (10 µM) for 6 h. After incubation, the culture medium was removed, and cells were washed with PBS, fixed, and permeabilized with paraformaldehyde (4%) and Triton X-100 (0.1%) for 10 min. subsequent incubation. Furthermore, cells were washed with PBS, mounted over a glass slide, and subjected to laser scanning confocal microscopic analysis.

Detection of hydroxyl radicals by terephthalic acid

Terephthalic acid (0.5 mM) and IOC-4-Z (100 µM) were mixed and subjected to irradiation for 20 minutes. After that, the fluorescence intensity of 2-hydroxy terephthalic acid was measured at 410 nm using Synergy H1 BioTek microplate reader by using excitation wavelength 325 nm.

Compounds	λ_{abs}/nm	λ_{em}/nm	PLQY (%)
IOC-1-Z	362	ND	ND
IOC-2-Z	405	548	16.81 ± 0.013
IOC-3-Z	425	560	16.90 ± 0.026
IOC-4-Z	401	550	94.11 ± 0.038
IOC-4-E	401	550	15.93 ± 0.022

Table S6. Photophysical properties such as absorbance (30 μM) in DMSO, emission in the solid state, and PLQY was measured after preparing thin films of IOCs in ethanol solvent. (ND-Not determined)

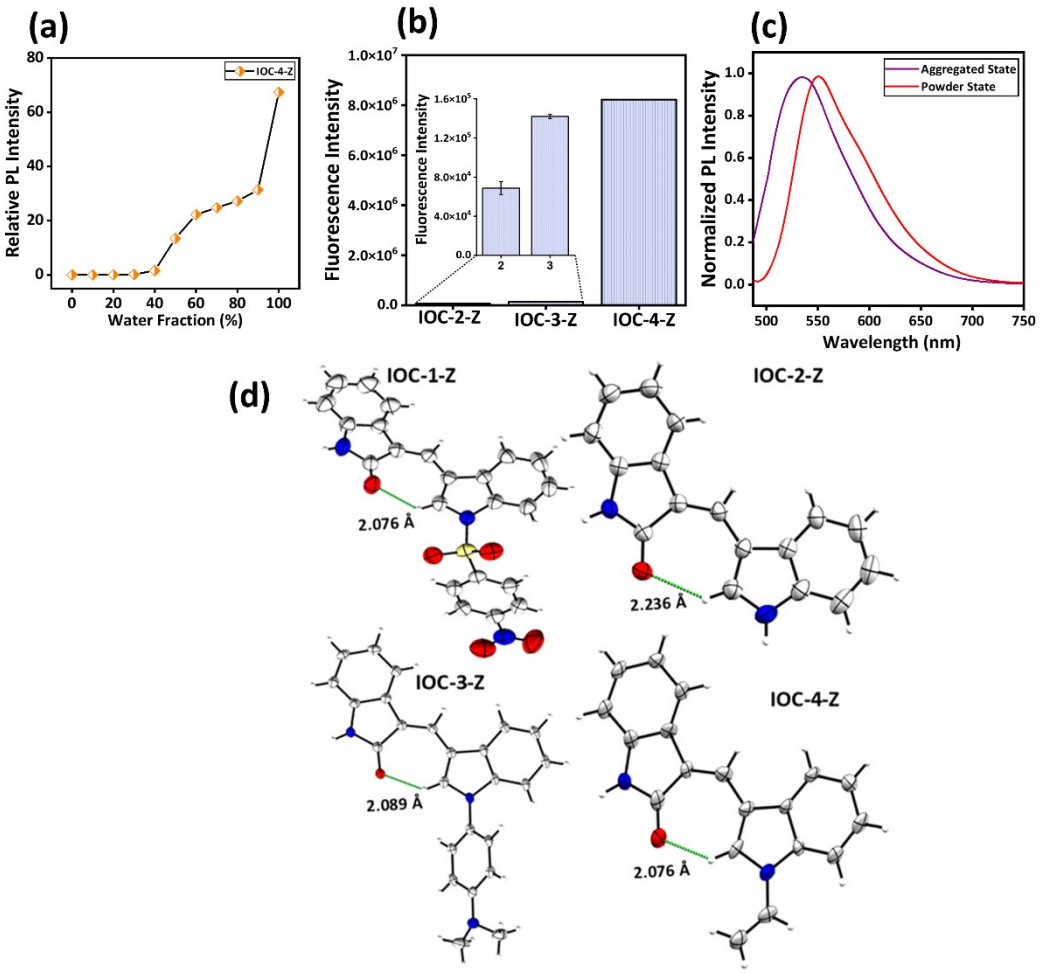

Fig. S2 (a) The fluorescence intensity enhancement of IOC-4-Z at different DMSO and water fractions. (b) Fluorescence intensity comparison of IOC-4-Z with IOC-3-Z and IOC-2-Z. (c) The fluorescence emission spectrum of IOC-4-Z under solution and powder state. (d) Crystal structure representation of all IOCs along with hydrogen bonding interactions.

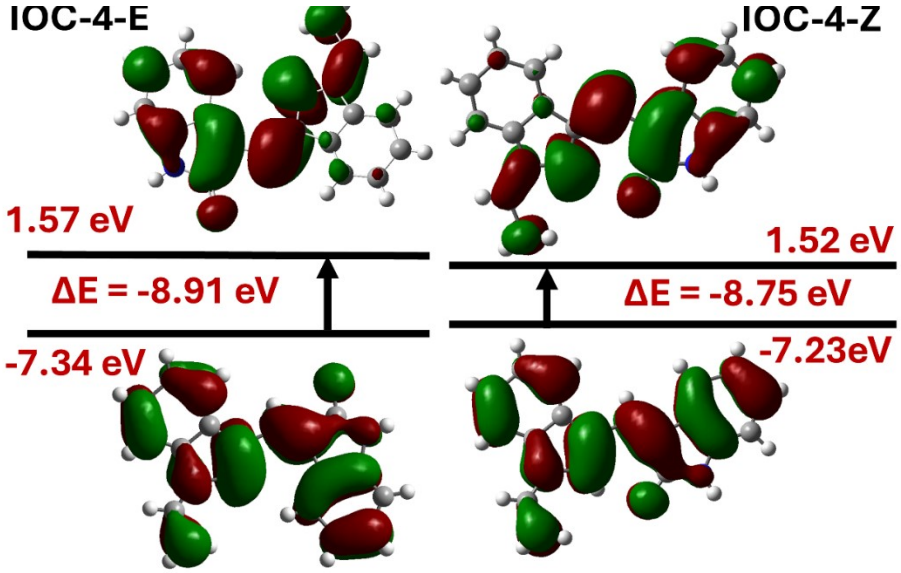

Fig. S3 Density functional theory analysis for the calculation of the HOMO-LUMO energy gap between IOC-4-Z and IOC-4-E.

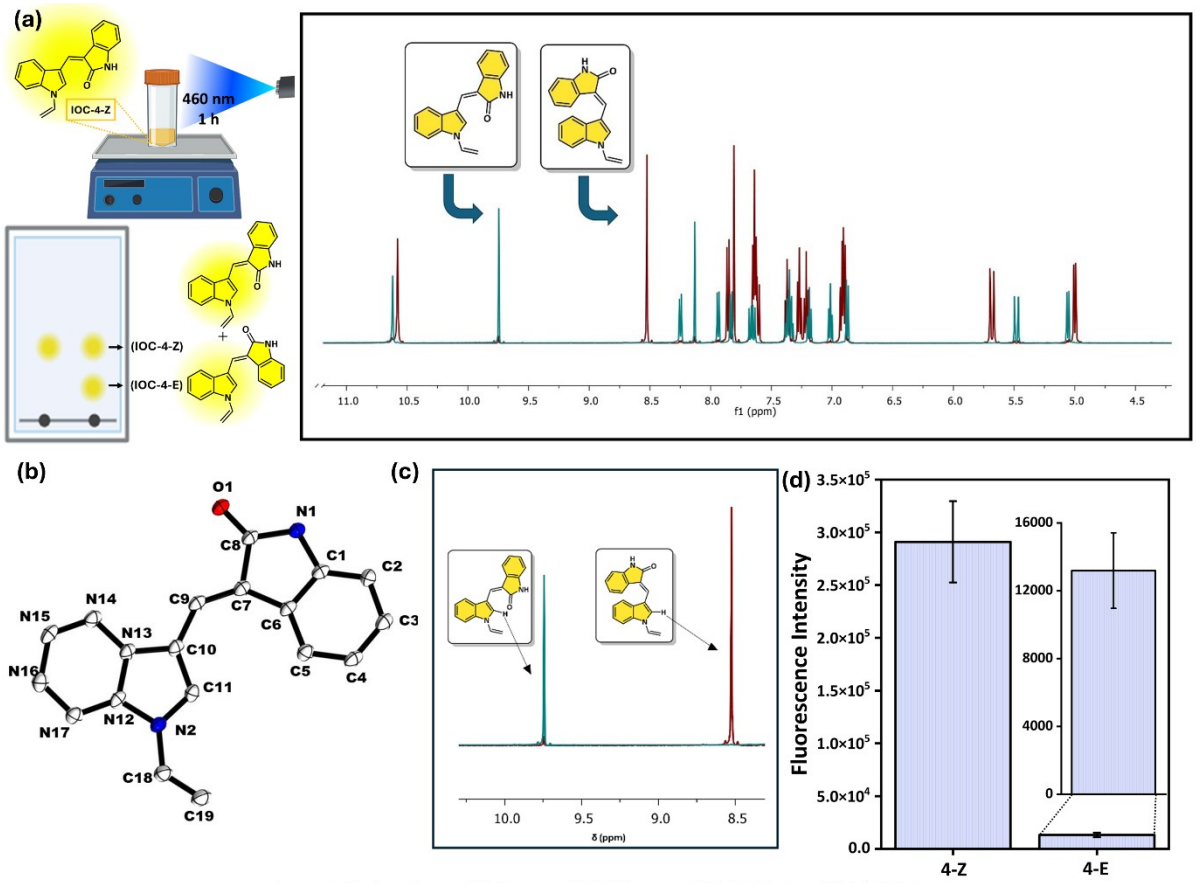

Fig. S4 a) Superimposed ^{1}H-NMR spectrum of IOC-4-Z with IOC-4-E after isolation. b) The crystal structure of IOC-4-E was obtained from X-ray diffraction analysis. c, d) Change in the ^{1}H-NMR chemical shift and fluorescence intensity of IOC-4-Z and IOC-4-E due to the presence and absence of intramolecular hydrogen bonding.

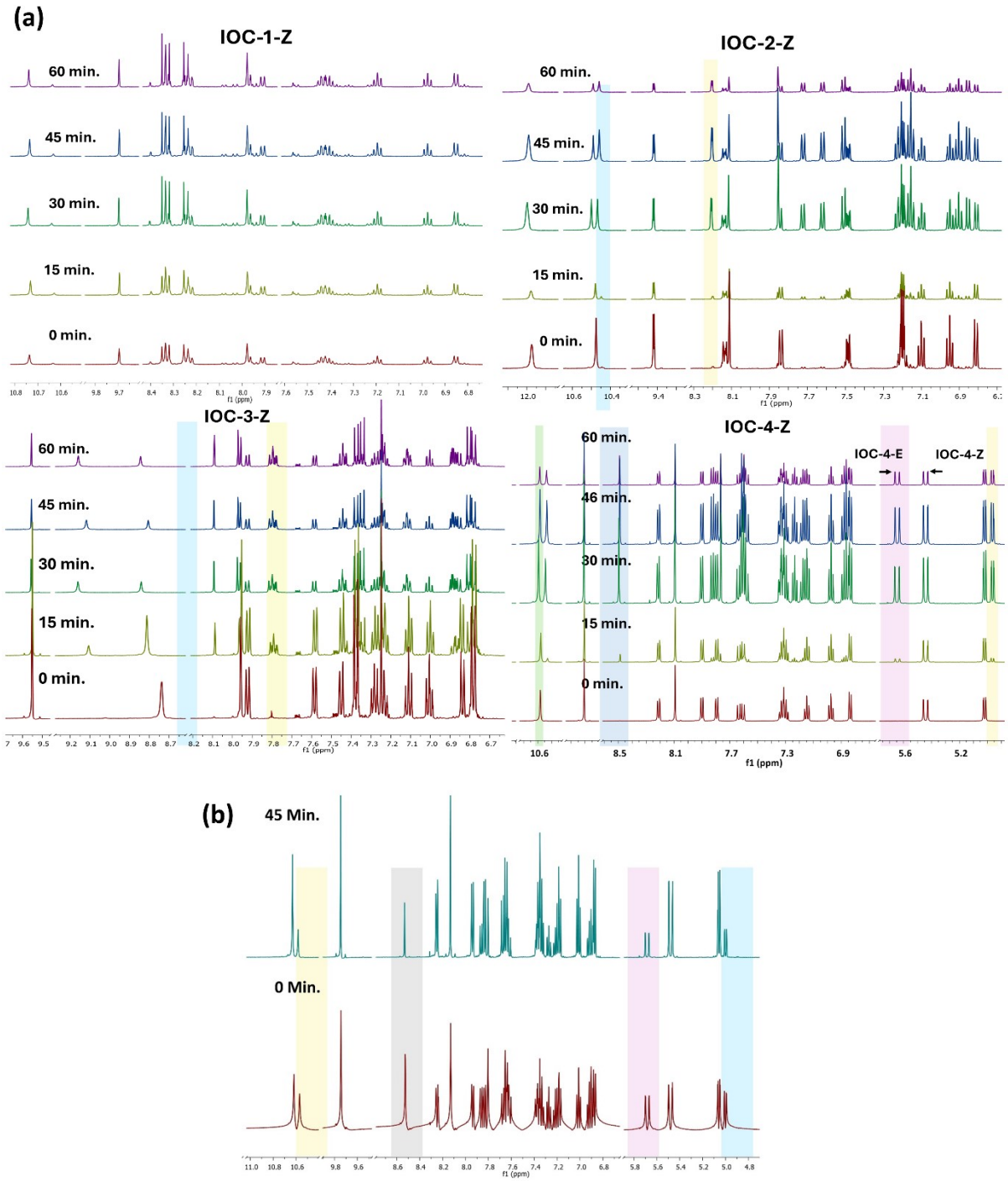

Fig. S5 a) Time-dependent NMR studies for Z-E photoisomerization of synthesized IOCs using 456 nm light irradiation. b) NMR analysis of E-Z transformations of photoirradiated (456 nm) IOC-4-Z using 365 nm light exposure.

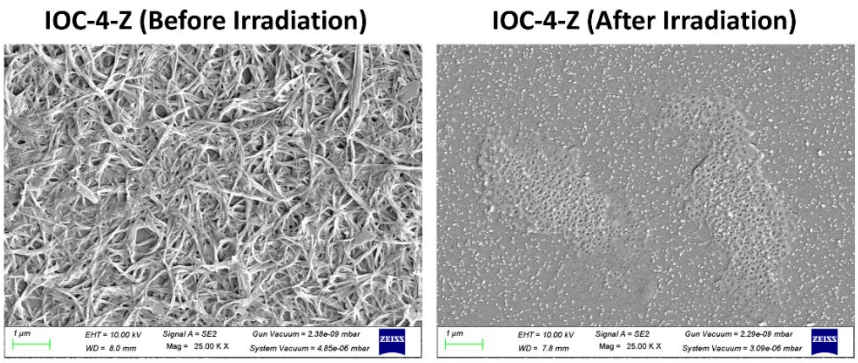

Fig. S6 Scanning electron microscope images of IOC-4-Z before and after irradiation.

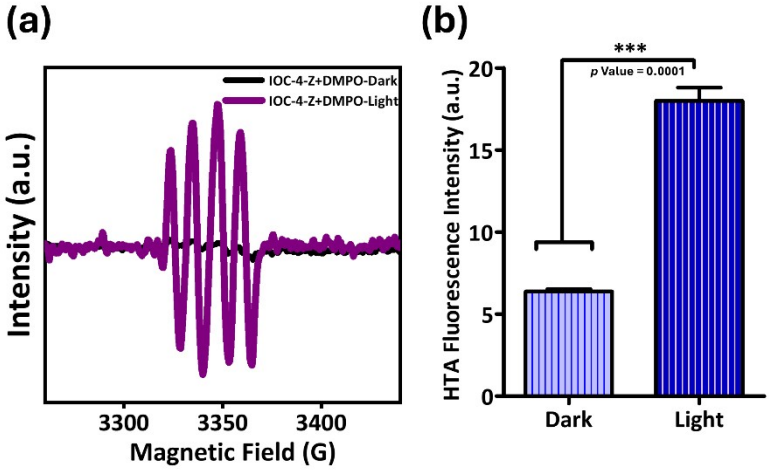

Fig. S7 (a) EPR spectrum of IOC-4-Z (200 µM) using spin trap DMPO (30 mM) under dark and light irradiated conditions. (b) Terephthalic acid (0.5 mM) oxidation into hydroxy terephthalic acid (HTA) with IOC-4-Z (100 µM) under dark and light exposed conditions.

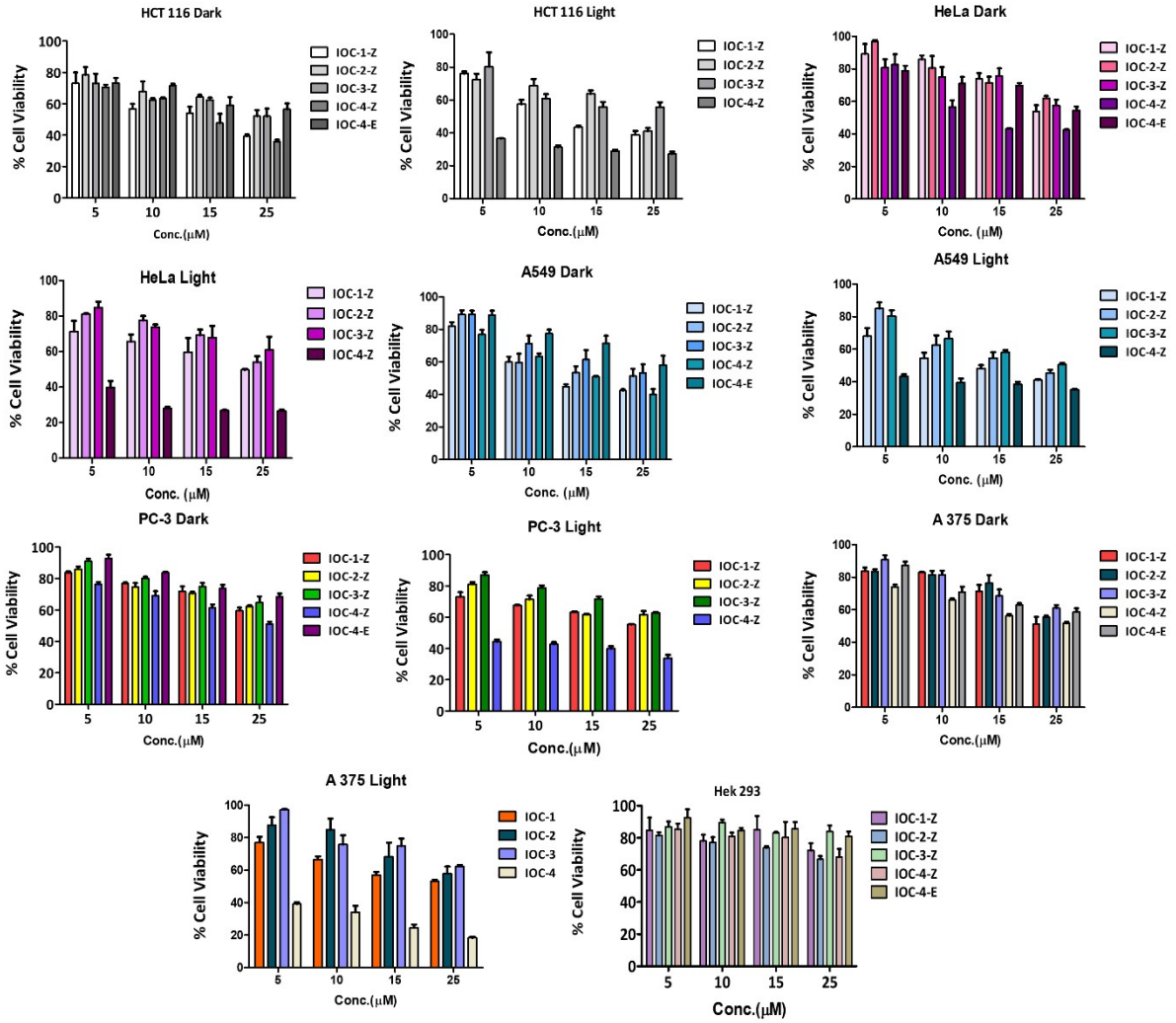

Fig. S8 Cell viability analysis of synthesized IOCs with different concentrations (5-25 µM) using various cancerous cell lines under dark and light-exposed conditions. Data represented as mean ± SD (n = 3). Statistical significance was evaluated using 1 sample t-test. *p < 0.1 **p < 0.01, ***p < 0.001.

Compounds	HCT 116		HeLa		A549		PC3		A375		HEK 293
	Dark	Light	Dark	Light	Dark	Light	Dark	Light	Dark	Light	Dark
IOC-1-Z	15.79 ± 1.92	13.77 ± 1.87	28.59 ± 1.93	27.09 ± 2.33	15.51 ± 1.85	13.95 ± 1.88	43.11 ± 1.99	41.41 ± 2.00	28.13 ± 1.95	27.02 ± 1.93	> 100
IOC-2-Z	29.57 ± 2.16	21.25 ± 1.99	34.44 ± 2.06	33.08 ± 2.00	20.64 ± 2.04	18.96 ± 1.92	47.02 ± 1.99	44.38 ± 2.16	35.06 ± 2.06	32.07 ± 2.16	> 100
IOC-3-Z	31.34 ± 2.25	26.95 ± 2.30	46.46 ± 2.64	42.96 ± 2.49	25.68 ± 1.99	23.93 ± 1.92	45.62 ± 2.00	45.48 ± 1.90	35.16 ± 1.97	36.68 ± 2.13	> 100
IOC-4-Z	14.35 ± 1.87	0.616 ± 2.56	14.84 ± 1.90	1.14 ± 2.80	16.42 ± 1.81	1.37 ± 2.92	27.58 ± 1.90	2.56 ± 2.49	25.95 ± 1.78	2.78 ± 2.16	90.01 ± 4.13
IOC-4-E	39.70 ± 2.44	-	37.42 ± 2.14	-	34.39 ± 2.06	-	50.15 ± 2.04	-	32.70 ± 2.00	-	> 100

Table S7. IC_{50} values for IOCs (µM) with different cell lines under dark (D) and light (L) irradiated conditions. Data represented as mean ± SD (n = 3). Statistical significance was evaluated using 1 sample t-test.

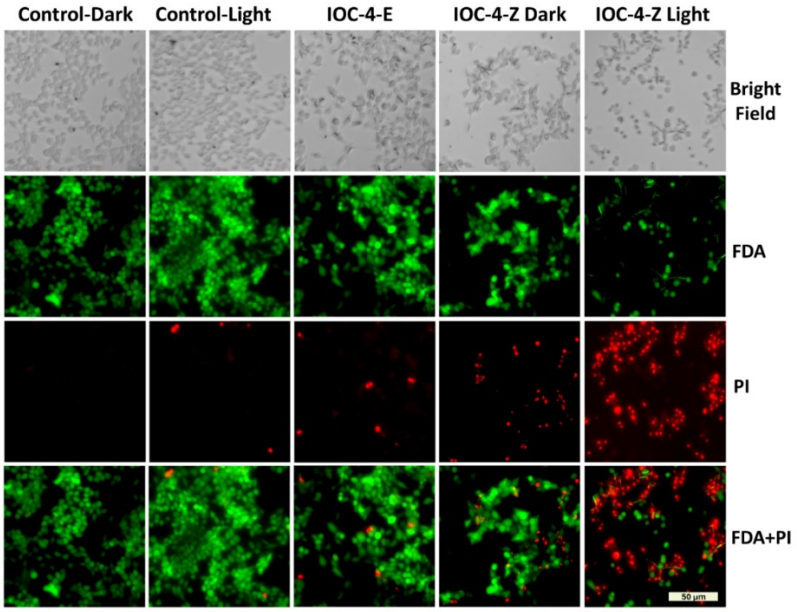

Fig. S9 FDA/PI co-staining analysis for the detection of live and dead cells before and after light irradiation. Magnification 20X, Scale bare: 50 µm.

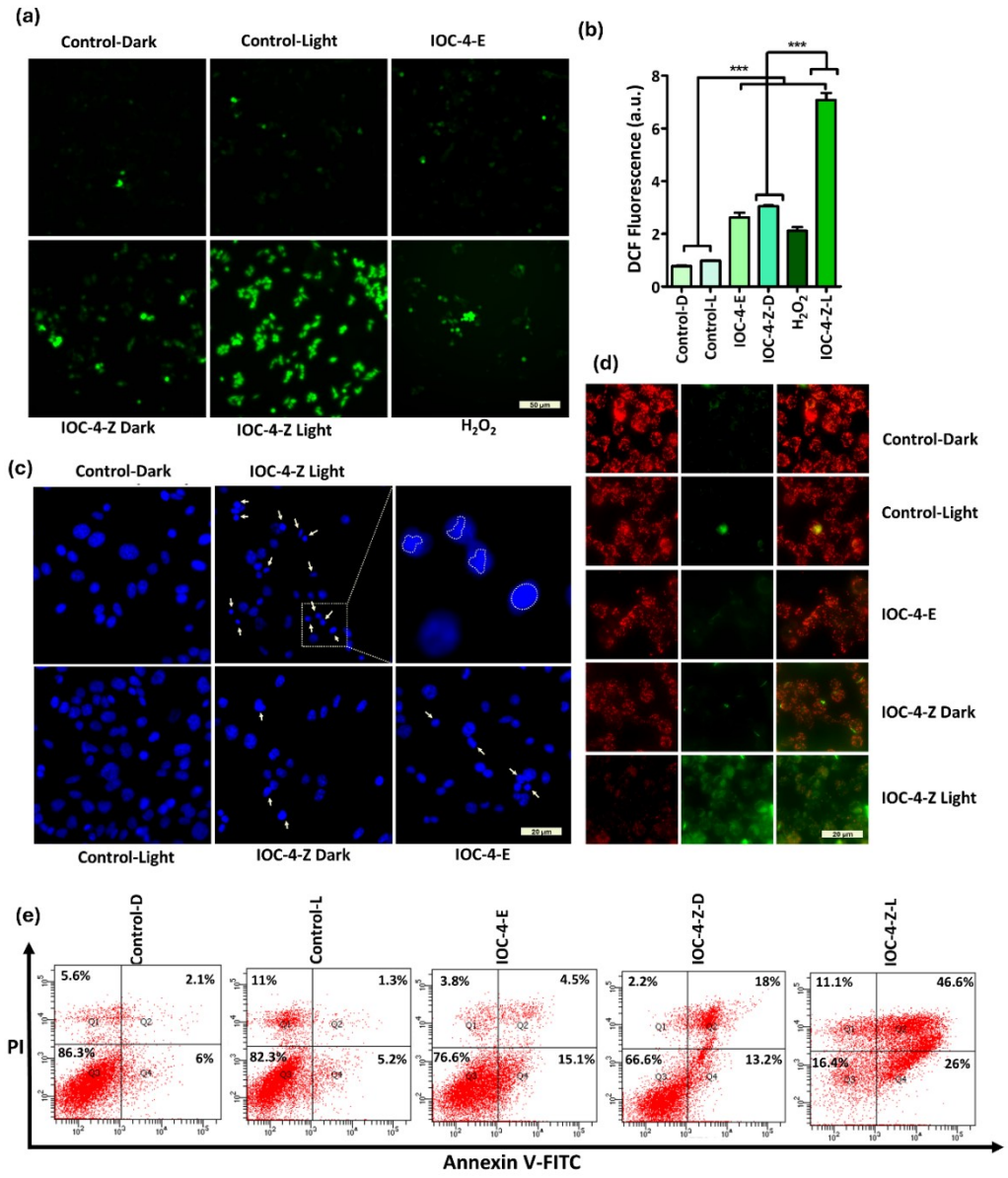

Fig. S10 a, b) DCFH-DA imaging and quantification analysis for ROS production under dark and light conditions. Magnification: 20X, Scale bar: 50 µm. Results obtained from quantitative analysis are presented as a fold increase with respect to the control. Data are mean ± SD (n = 3) in both panels; p values were calculated using one-way ANOVA with Tukey multiple comparison test; ***$p < 0.001$. c) DAPI staining analysis for DNA damage under dark and light conditions. Magnification: 60X, Scale bar: 20 µm. d) JC-1 staining analysis for the analysis of mitochondrial dysfunction under dark and light conditions. Magnification: 20X, Scale bar: 50 µ. e) Annexin V-FITC flow cytometric analysis for apoptosis detection under dark and light conditions.

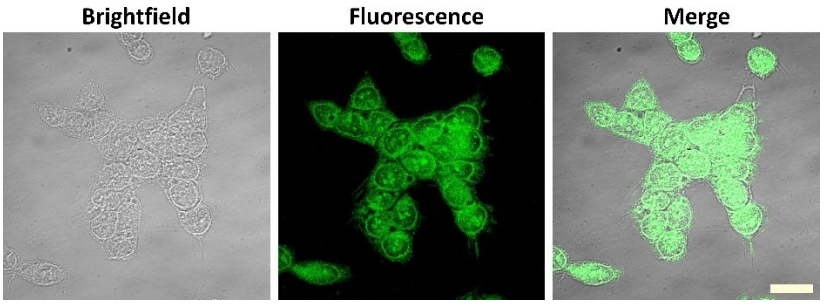

Fig. S11 Laser scanning confocal microscopic images of IOC-4-Z treated HCT 116 cells. Magnification: 100 X, Scale bar: 10 µm.

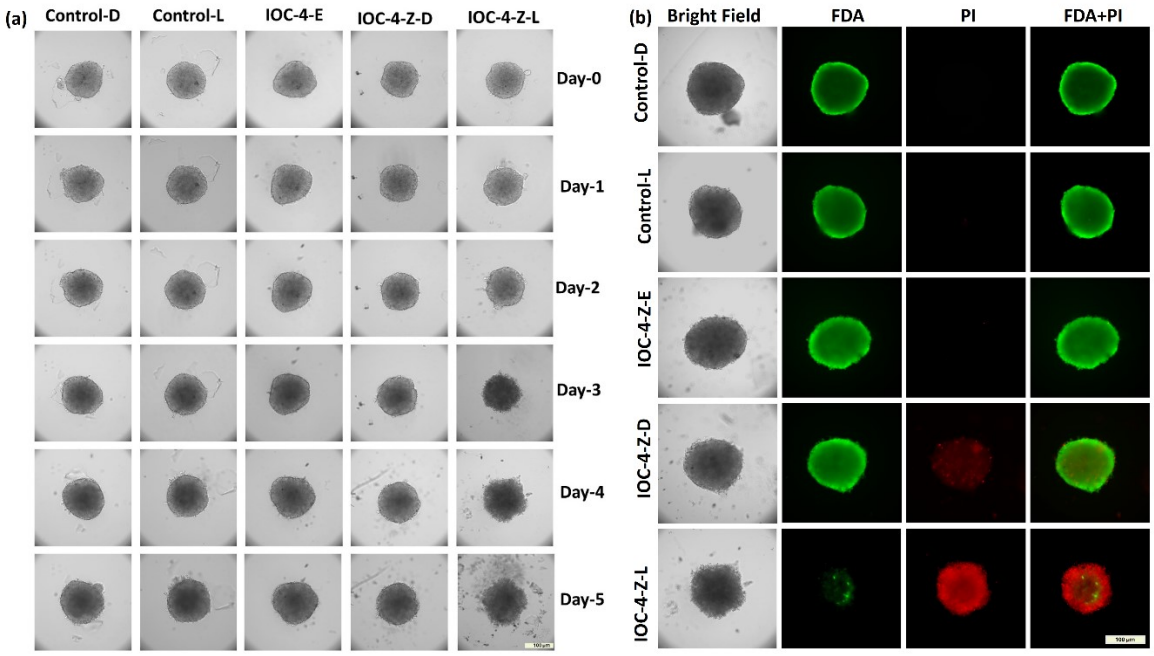

Fig. S12 a) Morphology changes and size reduction in HCT 116 3D spheroids after incubation with IOC-4-Z under dark and 456 nm light exposed conditions. Magnification: 10X, scale bar: 100 µm. b) FDA and PI co-staining analysis for the detection of live and dead cells in HCT 116 derived 3D-spheroids after IOC-4-Z incubation under dark and 456 nm light exposed conditions. Magnification: 10X, scale bar: 100 µm.

References:

1. B. Pettersson, V. Hasimbegovic, J. Bergman, *J. Org. Chem*., 2011, **76**, 1554-1561.
2. X. Liu, A. A. Flores, L. Situ, W. Gu, H. Ding, H. R. Christofk, W. E. Lowry, M. E. Jung, *J. Med. Chem*., 2021, **64**, 2046-2063.
3. K. Tyagi, R. Kumar, V. Venkatesh, *ChemMedChem*, 2025, e202400849
4. K. Tyagi, R. Kumar, V. Venkatesh, *Org. Biomol. Chem.,* 2023, **21**, 4455-4464.
5. V. Saini, K. Tyagi, R. Kumari, V. Venkatesh, *Chem Commun*., 2024, **60**, 12593-12596.

^{1}H NMR spectrum of aldehyde 1 (In $CDCl_3$)

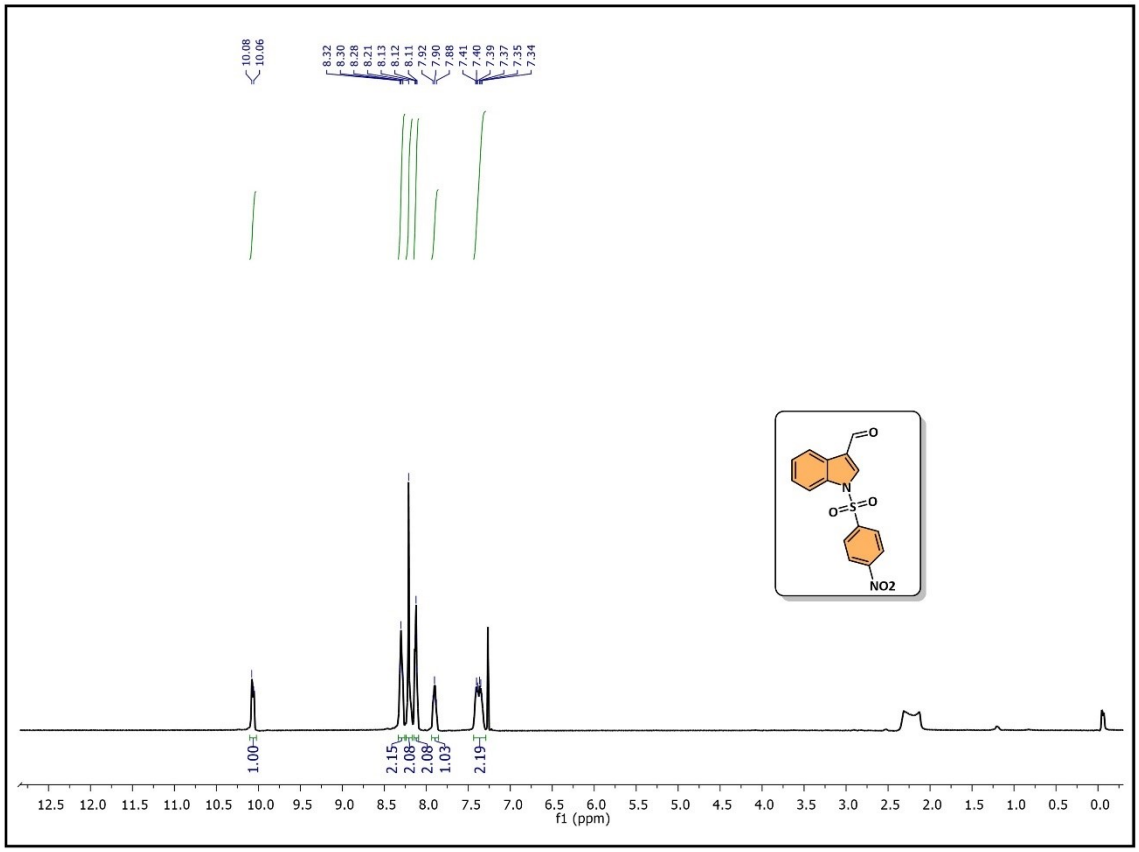

^{13}C NMR spectrum of aldehyde 1 (In $CDCl_3$)

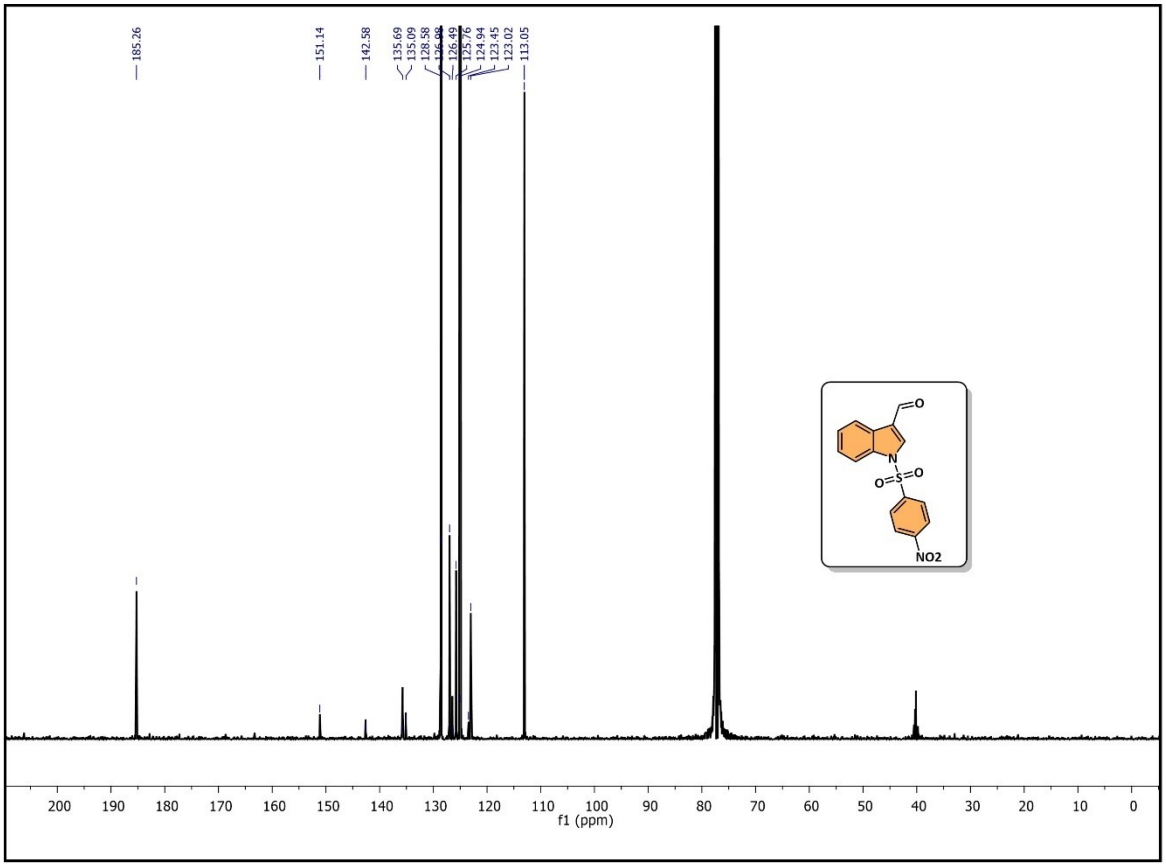

^{1}H NMR spectrum of aldehyde 2 (In $CDCl_3$)

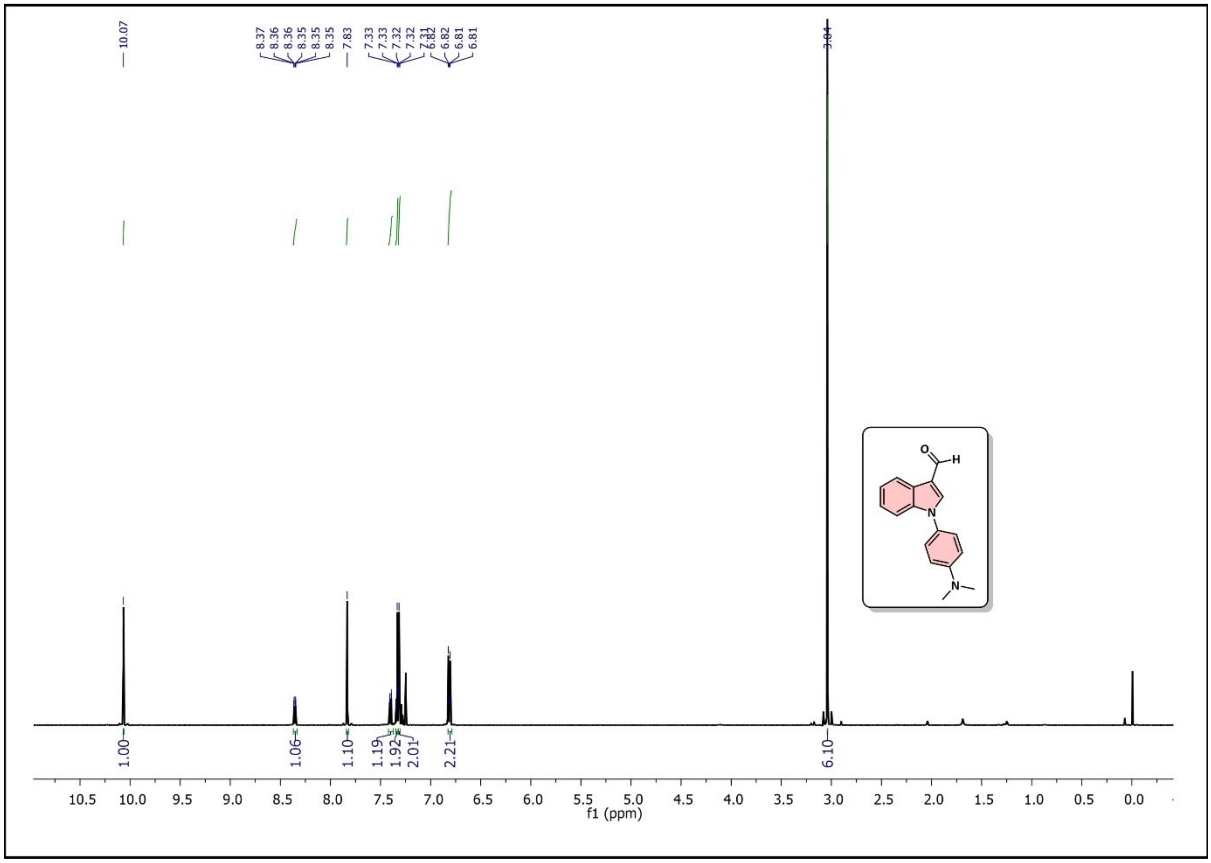

^{13}C NMR spectrum of aldehyde 2 (In $CDCl_3$)

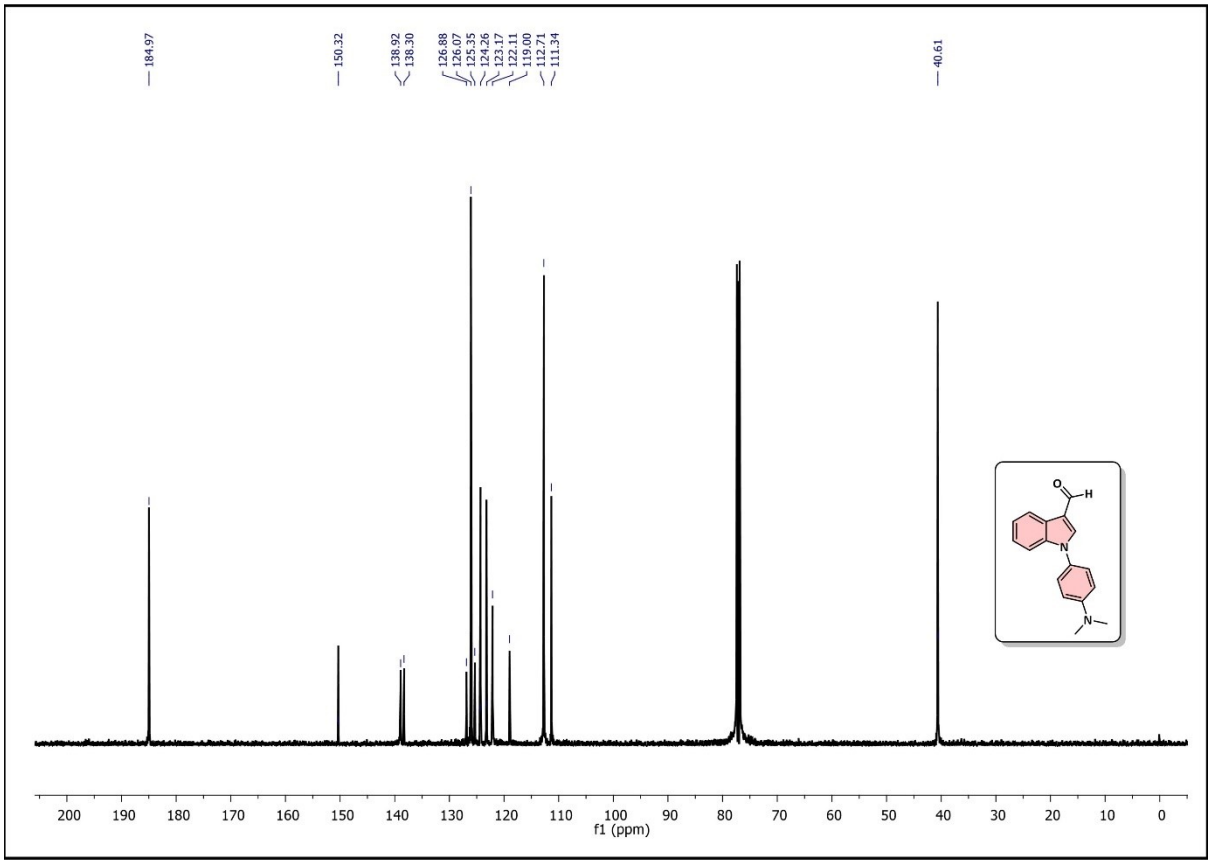

HRMS spectrum of aldehyde 2

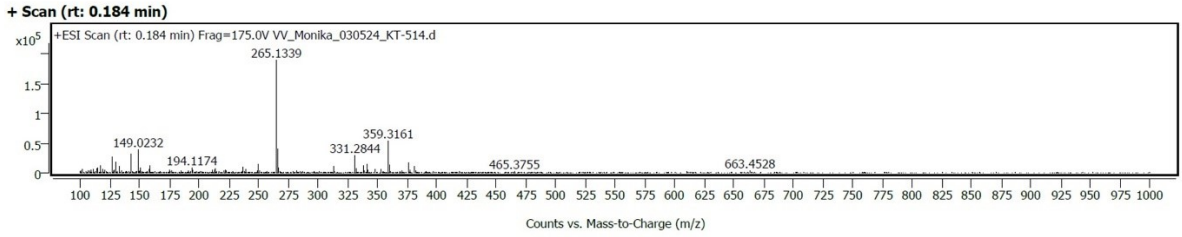

^{1}H NMR spectrum of aldehyde 3 (In $CDCl_3$)

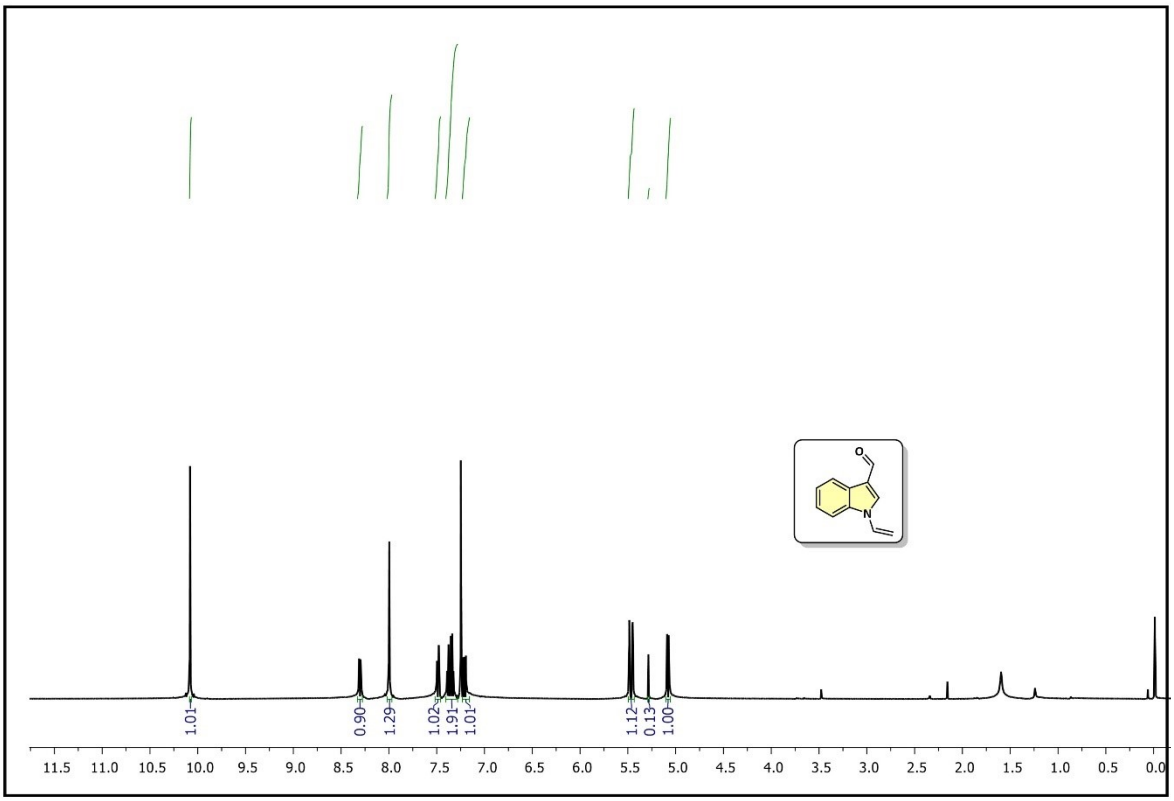

^{13}C NMR spectrum of aldehyde 3 (In $CDCl_3$)

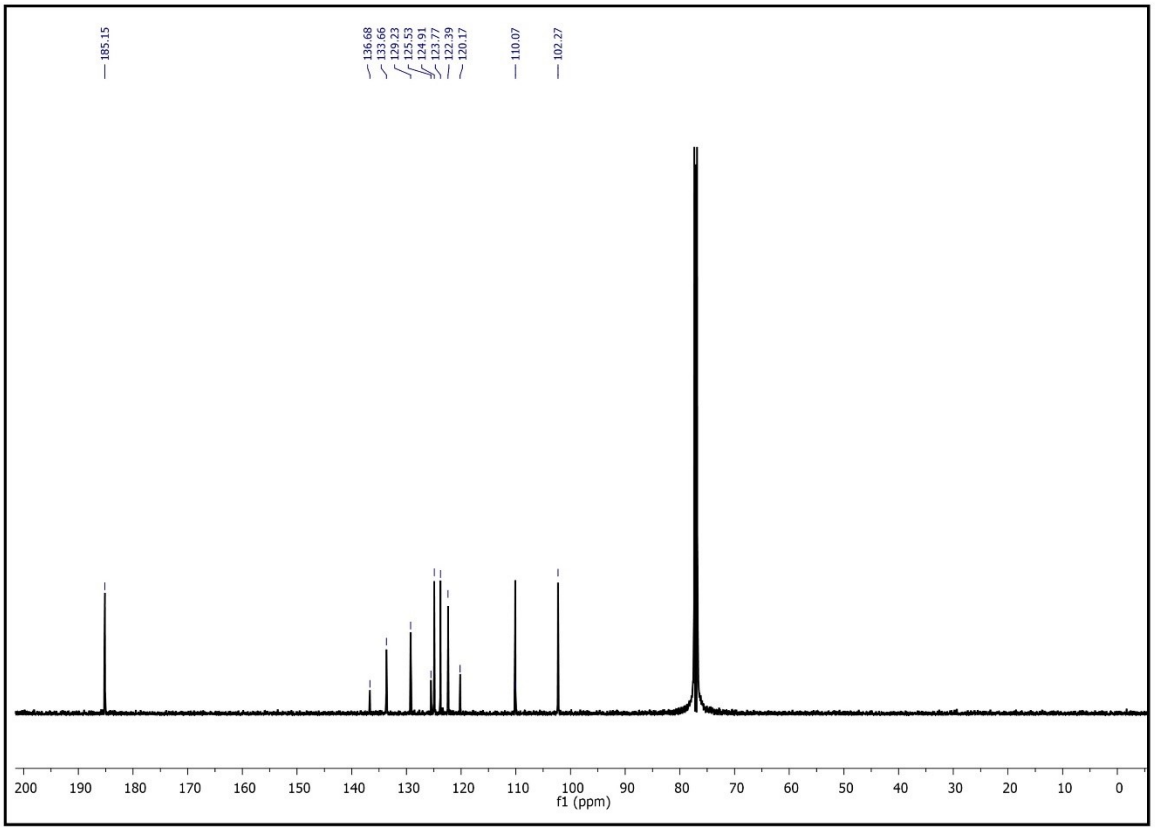

^{1}H NMR spectrum of IOC-1-Z (In DMSO-d_6)

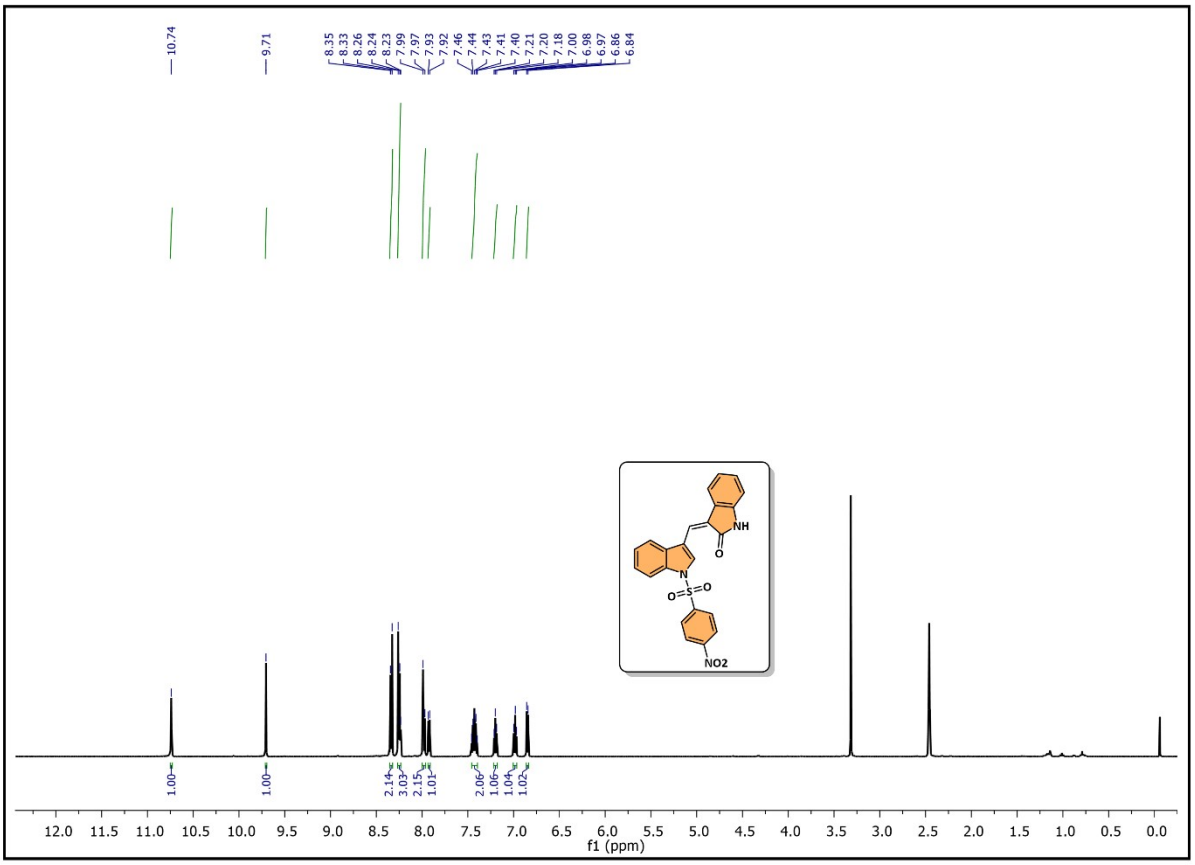

^{13}C NMR spectrum of IOC-1-Z (In DMSO-d_6)

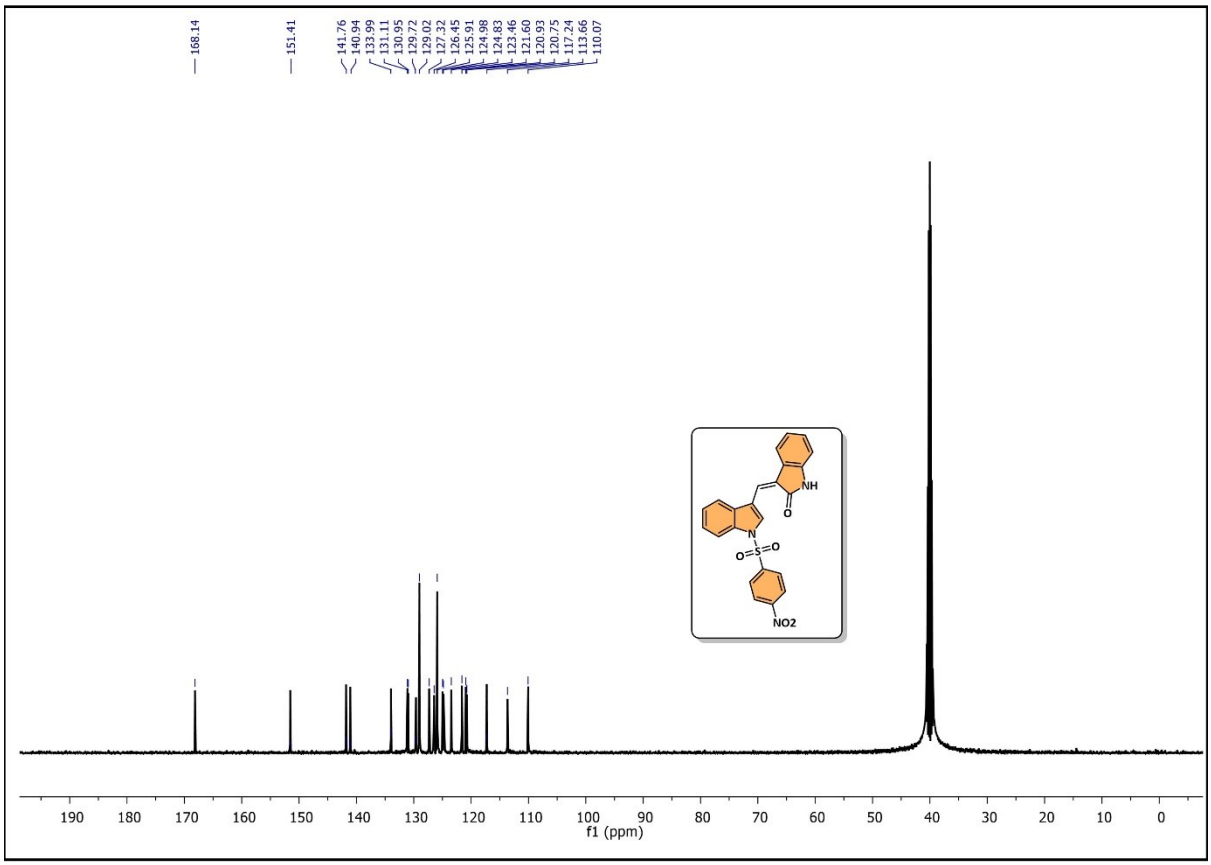

HRMS spectrum of IOC-1-Z

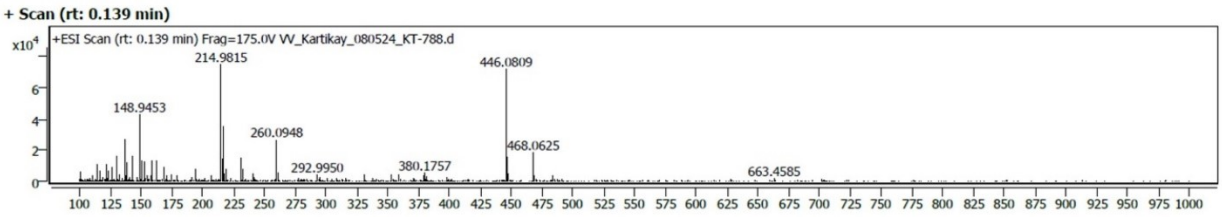

^{1}H NMR spectrum of IOC-2-Z (In DMSO-d_6)

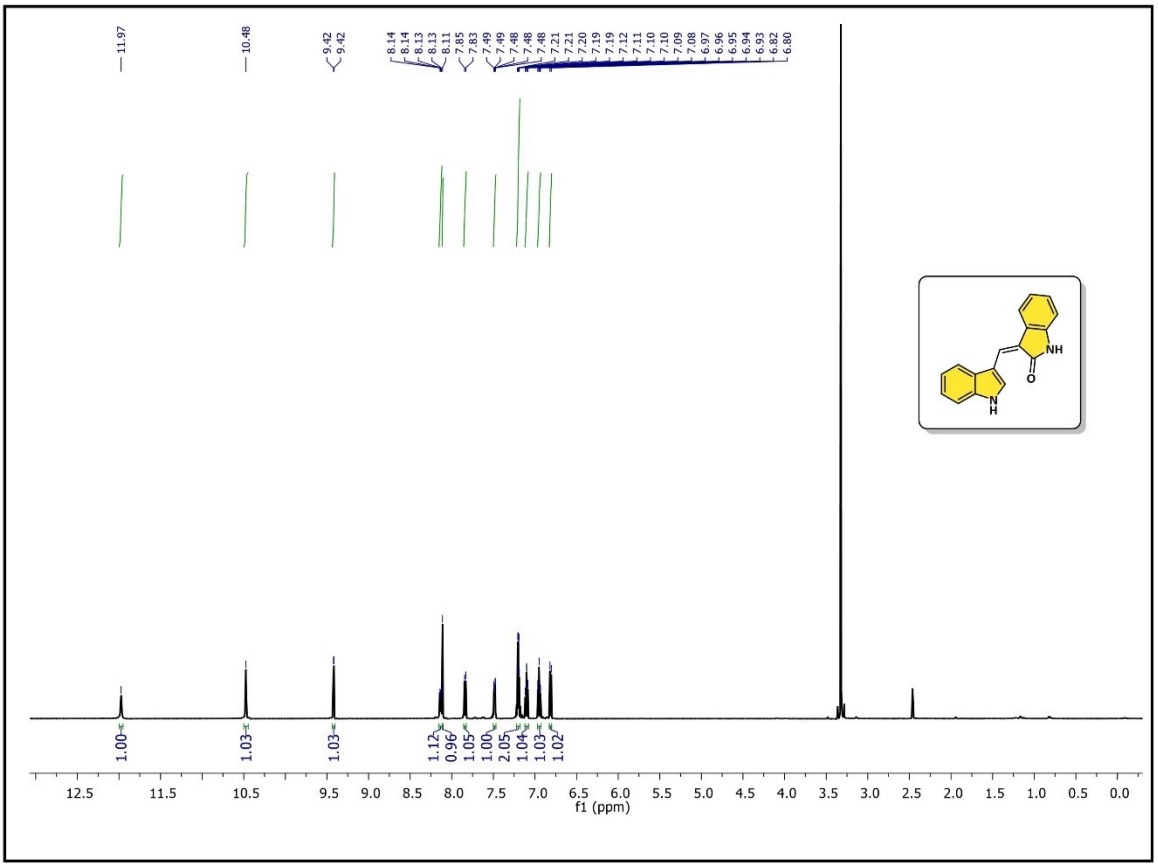

^{13}C NMR spectrum of IOC-2-Z (In DMSO-d_6)

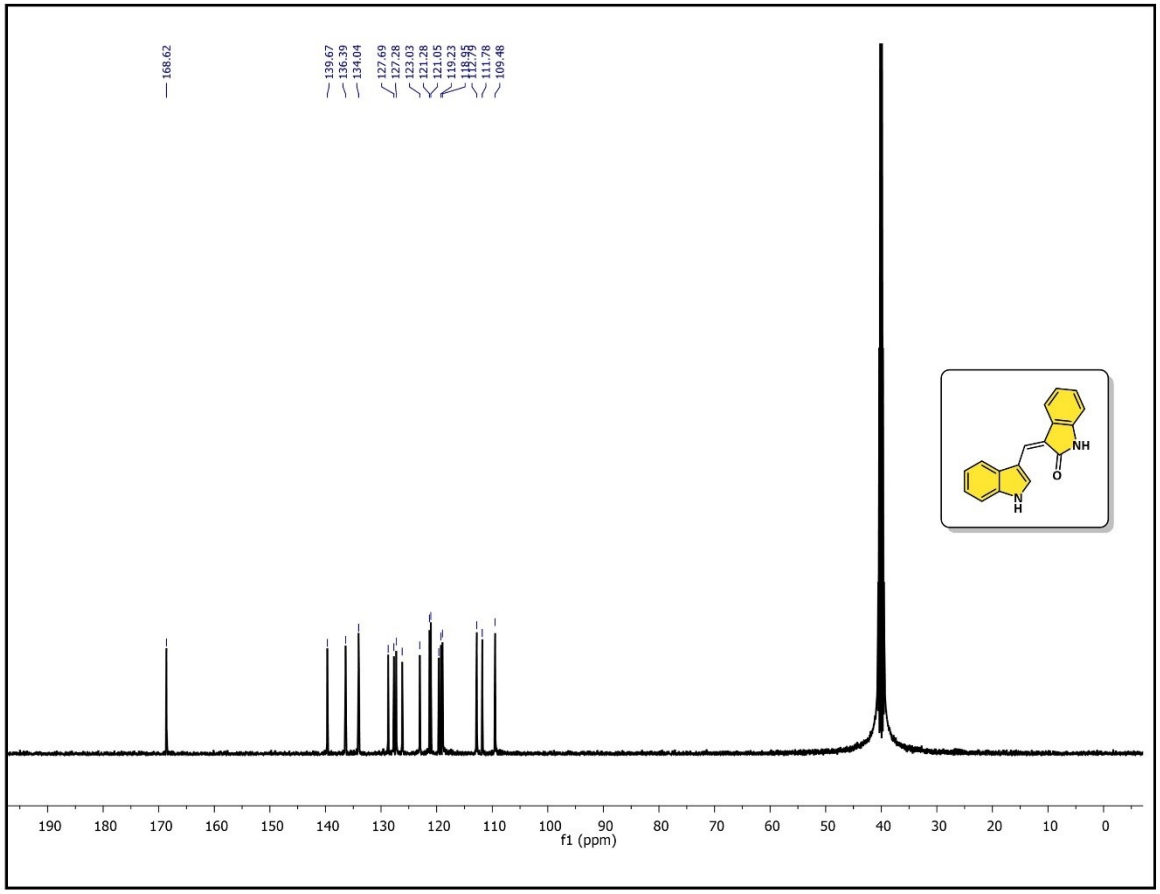

HRMS spectrum of IOC-2-Z

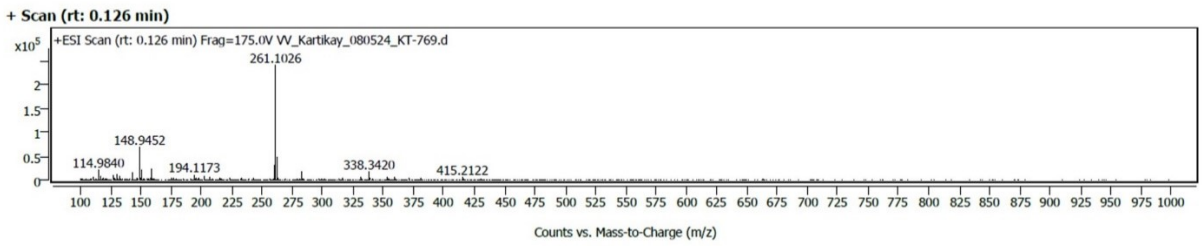

^{1}H NMR spectrum of IOC-3-Z (In $CDCl_3$)

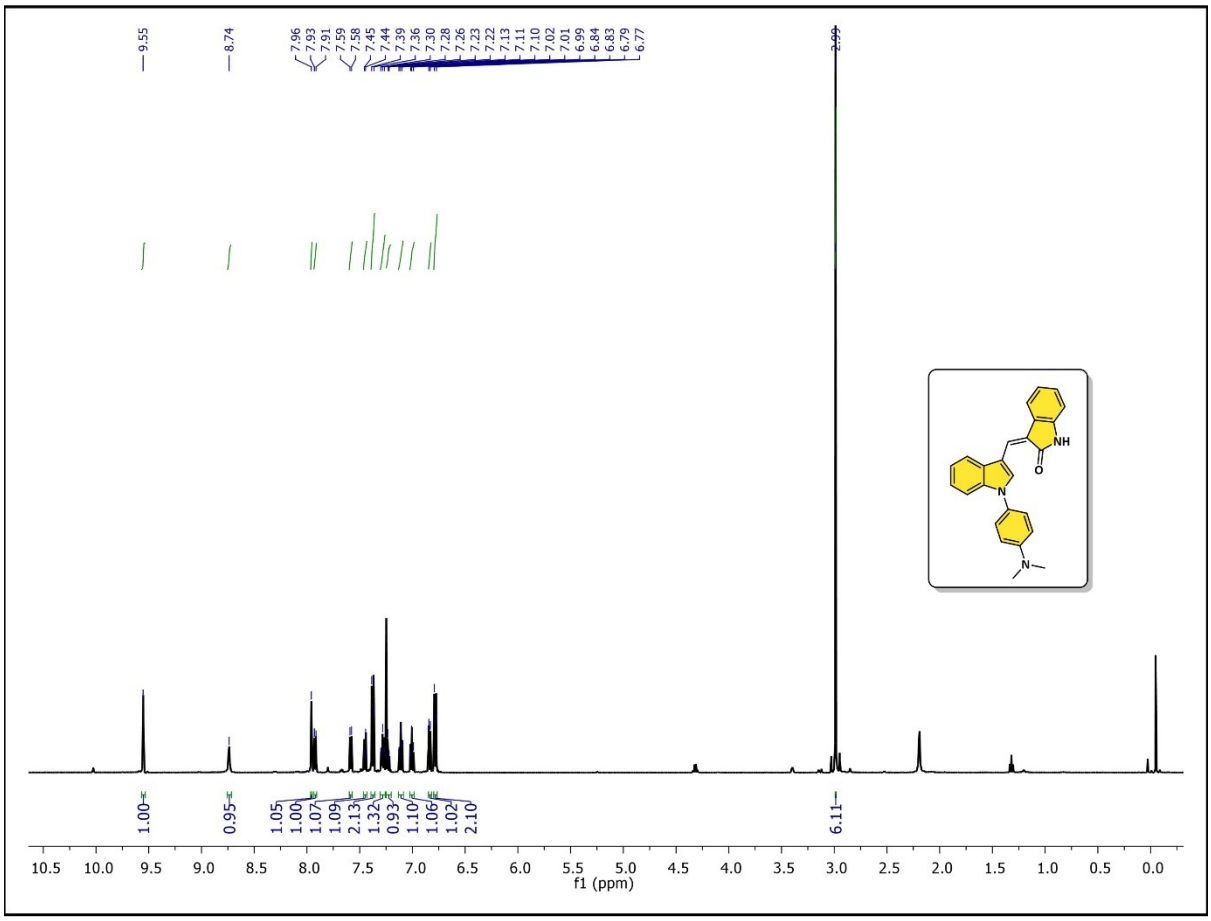

^{13}C NMR spectrum of IOC-3-Z (In $CDCl_3$)

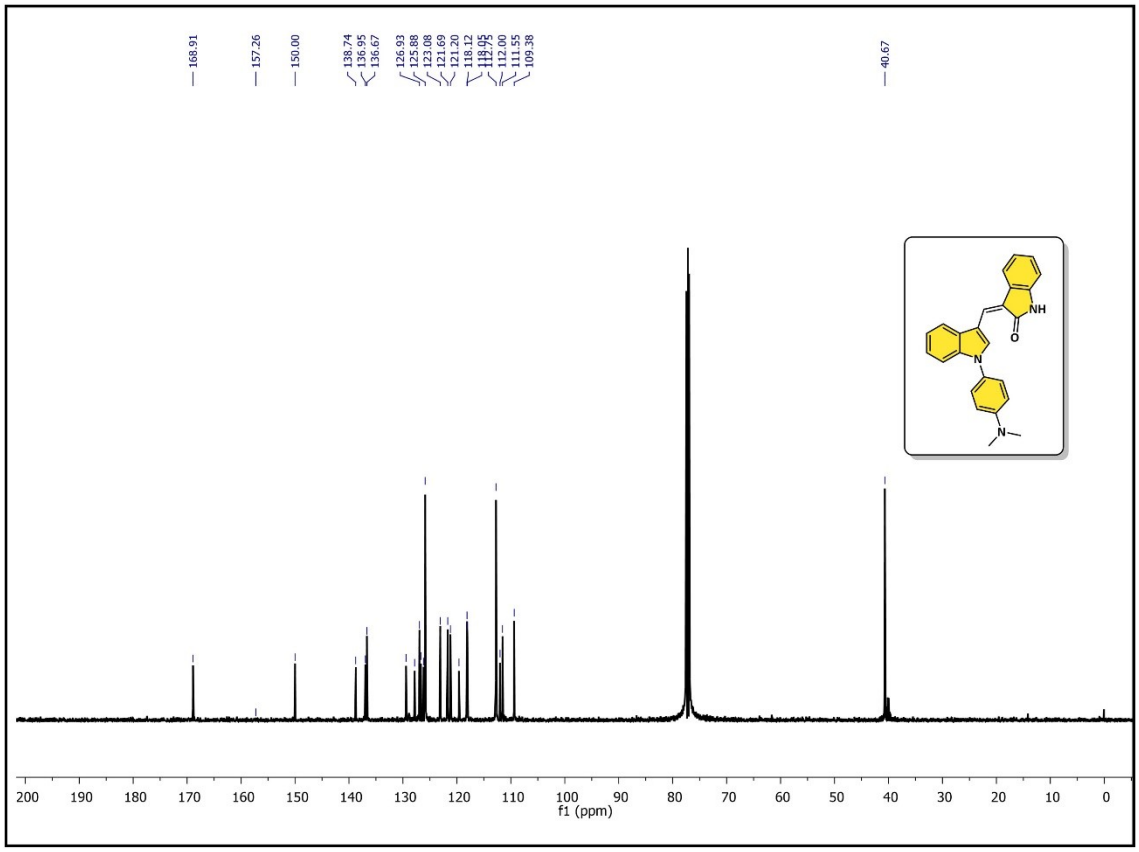

HRMS spectrum of IOC-3-Z

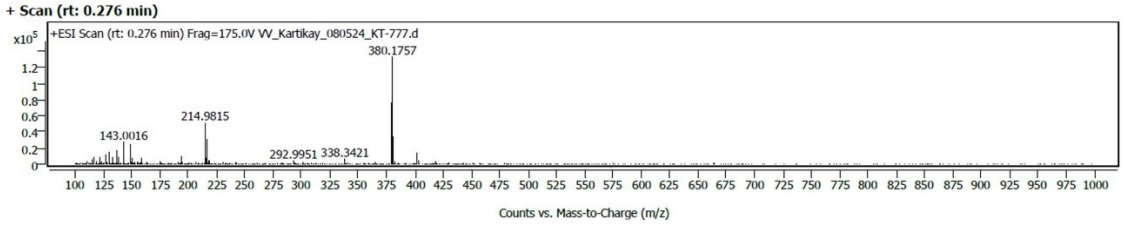

^{1}H NMR spectrum of IOC-4-Z (In DMSO-d_6)

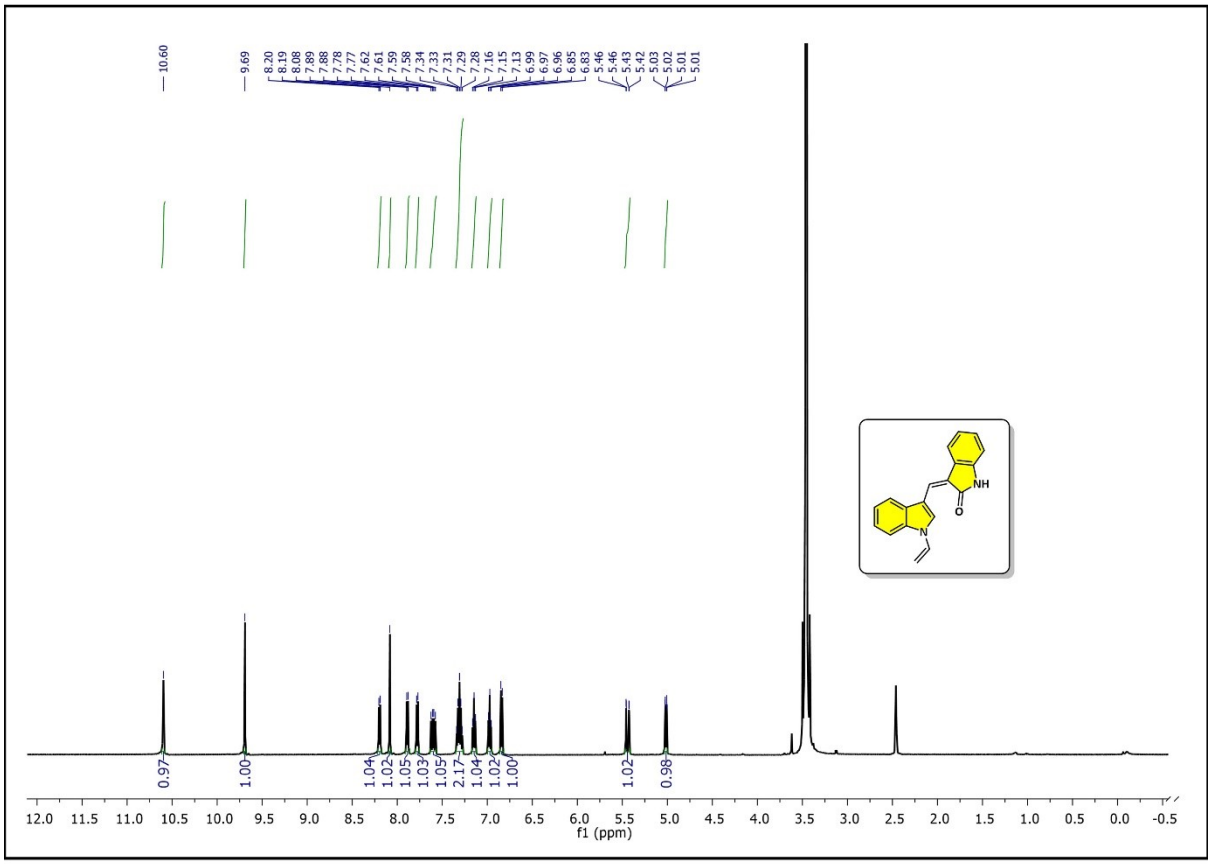

^{13}C NMR spectrum of IOC-4-Z (In DMSO-d_6)

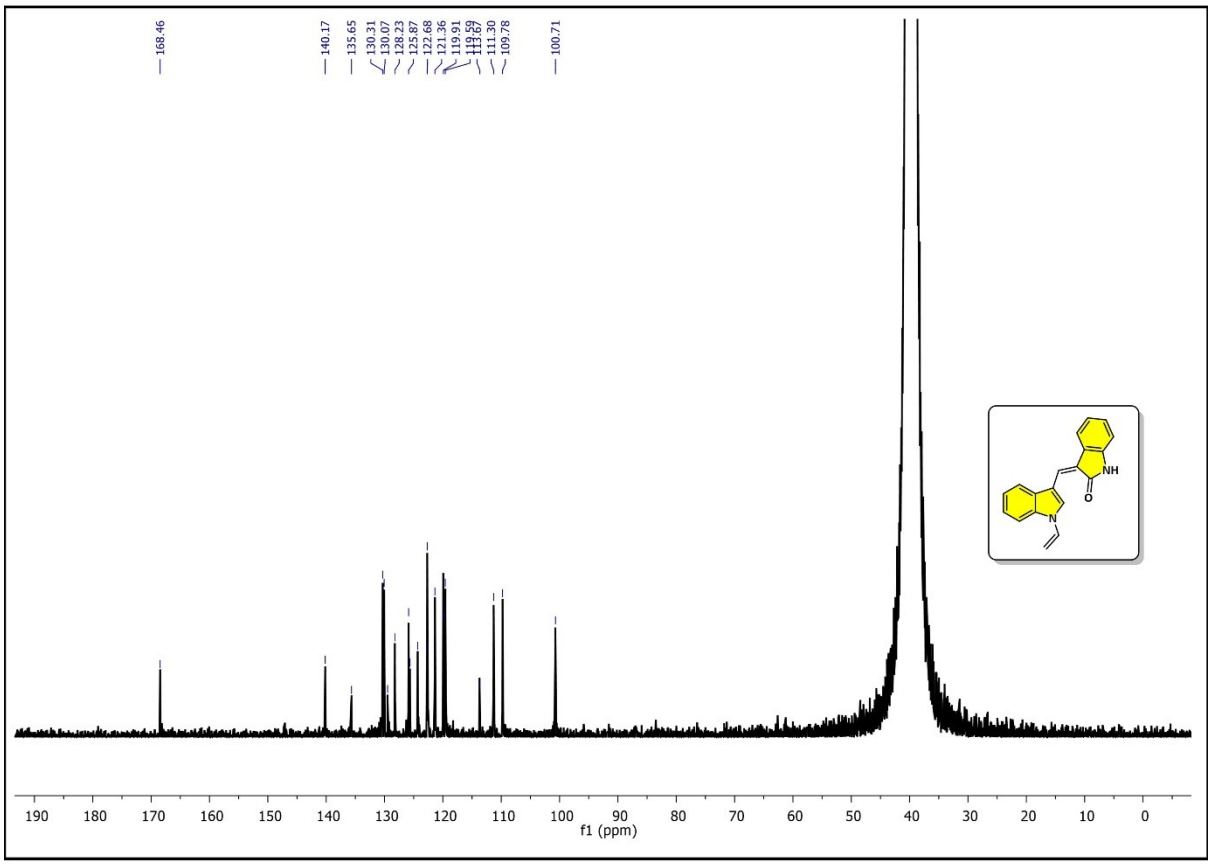

HRMS spectrum of IOC-4-Z

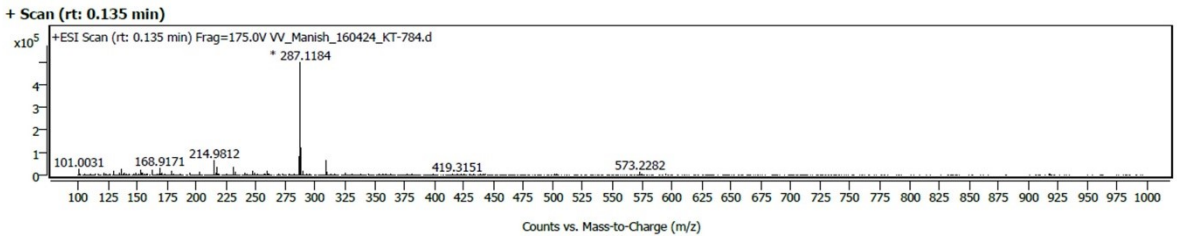

^{1}H NMR spectrum of IOC-4-E (In DMSO-d_6)

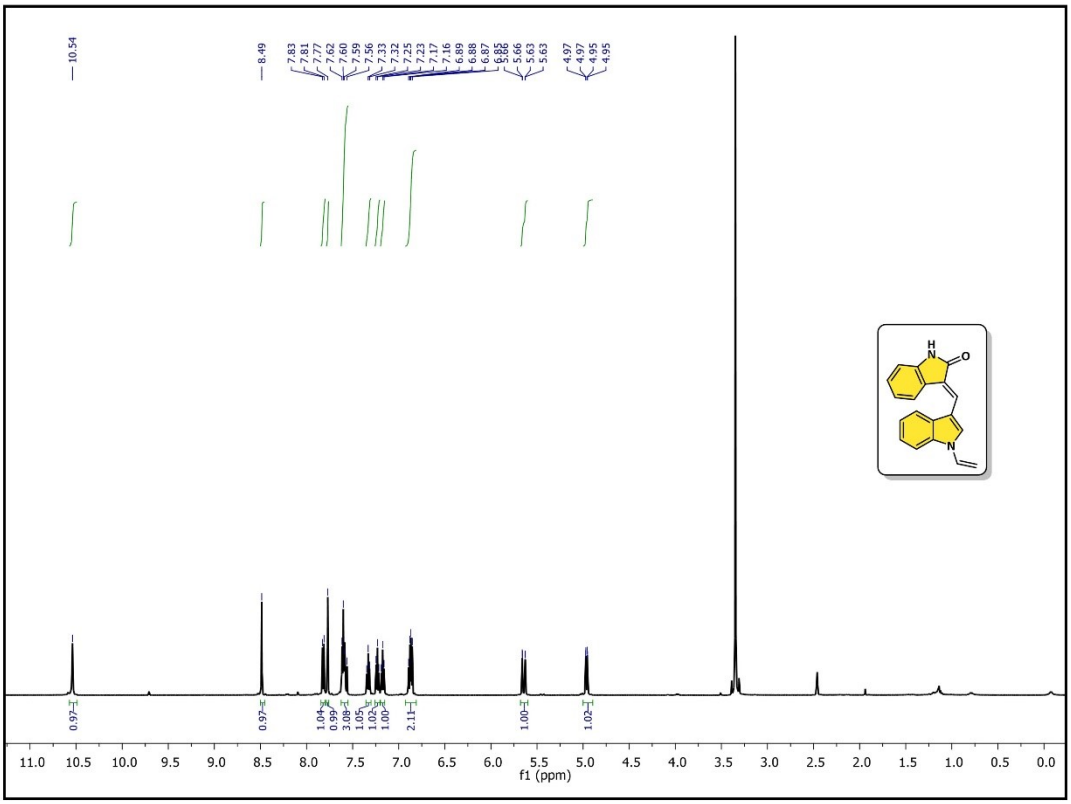

^{13}C NMR spectrum of IOC-4-E (In DMSO-d_6)

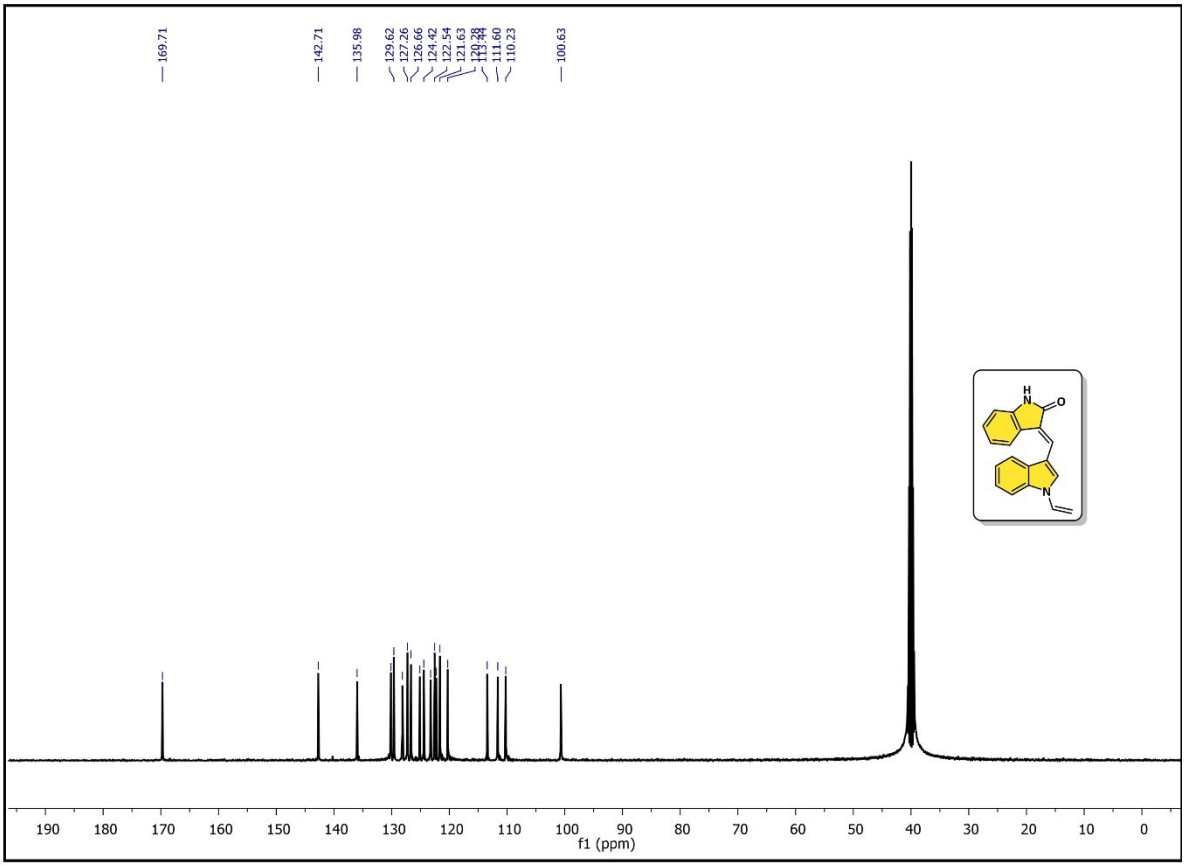

HRMS Spectrum of IOC-4-E